THE JOURNAL OF BIOLOGICAL CHEMISTRY VOL. 288, NO. 45, pp. 32539–32552, November 8, 2013

A Nondiscriminating Glutamyl-tRNA Synthetase in the *Plasmodium* Apicoplast

*THE FIRST ENZYME IN AN INDIRECT AMINOACYLATION PATHWAY**

Received for publication, August 6, 2013, and in revised form, September 23, 2013 Published, JBC Papers in Press, September 26, 2013, DOI 10.1074/jbc.M113.507467

Boniface M. Mailu[‡], Gowthaman Ramasamay[‡], Devaraja G. Mudeppa[§], Ling Li[‡], Scott E. Lindner[‡1], Megan J. Peterson[‡2], Amy E. DeRocher[‡], Stefan H. I. Kappe[‡¶], Pradipsinh K. Rathod[§¶], and Malcolm J. Gardner[‡¶3]

From the [‡]Seattle Biomedical Research Institute, Seattle, Washington 98109, the [§]Department of Chemistry, University of Washington, Seattle, Washington 98195-1700, and the [¶]Department of Global Health, University of Washington, Seattle, Washington 98195

Background: *Plasmodium* apicoplast protein synthesis is essential, but few apicoplast tRNA synthetases have been characterized.
Results: Apicoplast glutamyl-tRNA synthetase aminoacylates $tRNA^{Glu}$ and $tRNA^{Gln}$, is sensitive to a bacterial inhibitor, and is essential in blood stages.
Conclusion: Formation of apicoplast Gln-$tRNA^{Gln}$ is via indirect aminoacylation.
Significance: We demonstrate that the apicoplast glutamyl-tRNA synthetase is a potential drug target.

The malaria parasite *Plasmodium falciparum* and related organisms possess a relict plastid known as the apicoplast. Apicoplast protein synthesis is a validated drug target in malaria because antibiotics that inhibit translation in prokaryotes also inhibit apicoplast protein synthesis and are sometimes used for malaria prophylaxis or treatment. We identified components of an indirect aminoacylation pathway for Gln-$tRNA^{Gln}$ biosynthesis in *Plasmodium* that we hypothesized would be essential for apicoplast protein synthesis. Here, we report our characterization of the first enzyme in this pathway, the apicoplast glutamyl-tRNA synthetase (GluRS). We expressed the recombinant *P. falciparum* enzyme in *Escherichia coli*, showed that it is nondiscriminating because it glutamylates both apicoplast $tRNA^{Glu}$ and $tRNA^{Gln}$, determined its kinetic parameters, and demonstrated its inhibition by a known bacterial GluRS inhibitor. We also localized the *Plasmodium berghei* ortholog to the apicoplast in blood stage parasites but could not delete the *PbGluRS* gene. These data show that Gln-$tRNA^{Gln}$ biosynthesis in the *Plasmodium* apicoplast proceeds via an essential indirect aminoacylation pathway that is reminiscent of bacteria and plastids.

Malaria is a mosquito-borne disease caused by the apicomplexan parasite *Plasmodium*. The World Health Organization estimated that there are ~216 million malaria cases and 655,000 deaths annually, the latter mostly of young children in sub-Saharan Africa (1). Others recently reported that worldwide deaths are 2-fold higher (2). Resistance to most approved anti-malarials has been documented or is emerging (3), and despite encouraging progress against the disease with insecticide-impregnated bed nets and other tools, malaria control is difficult to maintain. This concern highlights the continual requirement for new anti-malarial drugs that are directed against novel targets.

The apicoplast (4) is a relict plastid and the remnant of an ancient secondary endosymbiotic event in which the eukaryotic progenitor of the malaria parasite engulfed a photosynthetic eukaryote. The circular 35-kb *Plasmodium* apicoplast genome (5) encodes components of the organelle's transcriptional and translational machinery (5–7) as well as the SufB protein involved in FeS cluster formation (8) and the ClpC protease. Most apicoplast proteins, however, are encoded by the nuclear genome and imported into the organelle post-translationally (9). Over 500 apicoplast-targeted proteins have been identified (10, 11), revealing apicoplast biosynthetic pathways for fatty acids (9, 12), isoprenoid precursors (13), and heme (14), as well as enzymes for tRNA modification (11) and lipoylation (15). Several of these pathways exhibit prokaryotic-like features and contain potential drug targets (11, 13, 16). Recent studies have shown that apicoplast isoprenoid precursor biosynthesis is essential in *P. falciparum* asexual stages (17), indicating that the pathway cannot be bypassed by salvage of lipids from the host and may be a good drug target in asexual stages. The type II fatty acid and heme biosynthetic pathways, however, are not essential in the asexual stages (16), and although not good targets for asexual stage chemotherapy, they may prove to be valuable prophylactic targets in liver stages (18).

Antibiotics that inhibit protein synthesis in prokaryotes can inhibit growth of blood stage parasites *in vitro* (19, 20) and possess anti-malarial properties *in vivo* (21, 22). Although slow acting against blood stage parasites and not used as first line

* This work was supported, in whole or in part, by National Institutes of Health Grant R21AI81097 from the NIAID (to M. J. G.) and Grants AI 093380 and AI 099280 (to P. K. R.). This work was also supported by the Murdock Trust, Seattle Biomedical Research Institute, and Puget Sound Partners for Global Health (to M. J. G.).
[1] Present address: Dept. of Biochemistry and Molecular Biology, Pennsylvania State University, W105 Millennium Science Complex, University Park, College Park, PA 16802.
[2] Present address: Institute of Molecular Biology, 1254 University of Oregon, Eugene, OR 97403.
[3] To whom correspondence should be addressed: Seattle Biomedical Research Institute, 307 Westlake Ave. N., Ste. 500, Seattle, WA 98109. Tel.: 206-256-7118; Fax: 206-256-7229; E-mail: malcolm.gardner@seattlebiomed.org.

drugs, antibiotics such as doxycycline have been used to treat patent blood stage infections that are resistant to fast acting drugs or when these drugs are unavailable (23). They are also used for prophylaxis against malaria transmitted by anopheline mosquitoes infected with *Plasmodium* sporozoites (24). Most, if not all, of these antibiotics inhibit apicoplast protein synthesis (25), suggesting that other processes that support this pathway might be useful drug targets.

Aminoacylated tRNAs synthesized by aminoacyl-tRNA synthetases (aaRSs)[4] are essential substrates for protein synthesis. Consequently, aaRSs have emerged as targets for new antibiotics (26). Mupirocin, for example, is a topical antibiotic already in clinical use, and other aaRS inhibitors such as the boronated antifungal compound AN2690 (27) are being developed. Aminoacylation in malaria parasites had been little studied despite its critical role in parasite biology and potential as a drug target, but studies describing the apicoplast (28) and cytoplasmic aspartyl-tRNA synthetases (29), lysyl-tRNA synthetases (30, 31), and tryptophanyl-tRNA synthetases (32, 33) were recently published.

The classical route for aminoacylated tRNA formation, direct aminoacylation, is catalyzed by aaRSs specific for each cognate amino acid:tRNA pair, but some aminoacylated tRNAs are made via alternative pathways. Most bacteria lack glutaminyl-tRNA synthetase (GlnRS) and produce Gln-tRNA^{Gln} via a two-step indirect aminoacylation pathway (34) shown as Reactions 1 and 2. First, tRNA^{Gln} is glutamylated by a nondiscriminating glutamyl-tRNA synthetase (GluRS). The misacylated Glu-tRNA^{Gln} is subsequently converted into Gln-tRNA^{Gln} by glutamyl-tRNA amidotransferase (Glu-AdT).

$$\text{L-Glutamate} + \text{ATP} + \text{tRNA}^{Gln} \rightleftharpoons \text{Glu-tRNA}^{Gln} + \text{AMP} + \text{PP}_i$$

REACTION 1

$$\text{L-Glutamine} + \text{ATP} + \text{Glu-tRNA}^{Gln} \rightleftharpoons \text{Gln-tRNA}^{Gln} + \text{L-Glutamate} + \text{ADP} + \text{P}_i$$

REACTION 2

The second step (Reaction 2) catalyzed by Glu-AdT is essential because the misacylated Glu-tRNA^{Gln} is toxic if it is not converted to Gln-tRNA^{Gln} by Glu-AdT (35).

By analyzing conserved apicoplast-targeted proteins in the genomes of several *Plasmodia* (10, 36, 37) and the related parasite *Theileria parva* (38), we noticed that both organisms encoded apicoplast-targeted GluRS and Glu-AdT enzymes but lacked an apicoplast-targeted GlnRS. We hypothesized that the apicoplast utilizes the indirect pathway for Gln-tRNA^{Gln} biosynthesis and that inhibition of this pathway might provide a new way to inhibit apicoplast protein synthesis. We began to explore these hypotheses by characterizing the first enzyme in the pathway, the apicoplast-targeted GluRS.

[4] The abbreviations used are: aaRS, aminoacyl-tRNA synthetase; ACP, acyl-carrier protein; GluRS, glutamyl-tRNA synthetase; Glu-SA, 5′-*O*-[*N*-(L-glutamyl)sulfamoyl]adenosine; GlnRS, glutaminyl-tRNA synthetase; Pb, *P. berghei*; Pf, *P. falciparum*; PPase, inorganic pyrophosphatase; AspRS, Glu-AdT, glutamyl-tRNA amidotransferase; Ni-NTA, nickel-nitrilotriacetic acid; For, forward; Rev, reverse; DHFR, dihydrofolate reductase; -TS, -thymidylate synthase.

EXPERIMENTAL PROCEDURES

Bioinformatics—A list of putative apicoplast-targeted proteins conserved in *Plasmodium falciparum*, *T. parva*, and *Toxoplasma gondii* was obtained from the supplementary information in Gardner *et al.* (38). Nucleotide or amino acid sequences of *Plasmodium* genes or proteins (10, 39) and those from other species were obtained from PlasmoDB (40), the Wellcome Trust Sanger Institute GeneDB website, or UniProt (41). Multiple sequence alignments were generated using tCoffee-Expresso (42) and formatted for display using ESPript (43) with SimilarityGlobalScore = 0.7, SimilarityDiffScore 0.5, SimilarityType = R (Risler), and Consensus = C. The phylogenetic tree was constructed using the tools provided on line (44). The "one-click" mode was used, employing MUSCLE (45) for sequence alignment and Gblocks (46), PhyML (47), and TreeDyn (48) for curation of the multiple sequence alignment and tree construction and rendering, respectively. The final tree was constructed using 200 bootstraps.

Isolation of the PfGluRS cDNA from Blood Stage Parasites—*P. falciparum* 3D7 asexual stage parasites (MRA-102, MR4 ATCC (BEI Resources), Manassas, VA) were cultured as described (49). Infected erythrocytes were lysed with 0.5% saponin (Sigma) and total RNA was isolated using TRIzol (Invitrogen). A cDNA of the PfGluRS gene (Pf3D7_1357200) was amplified by RT-PCR using the GR31_F primer (5′-GAGAGGAAATAGGTGTAATGT-3′), which maps 25 nucleotides 5′ to the predicted start codon and the reverse primer G33_R (5′-AAACTTAAATAGATTTTTCAAATGTAA-3′) that is complementary to the 3′ end of the predicted coding sequence. The resulting PCR product was cloned into the pCR-XL-TOPO vector (Invitrogen) and sequenced.

Expression and Purification of Mature PfGluRS in Wheat Germ Extracts—Two versions of the PfGluRS coding sequence were cloned for expression in wheat germ extracts. The native PfGluRS coding sequence (amino acids 78–574), minus the predicted apicoplast leader sequence (amino acids 1–77), was amplified from first strand cDNA using forward (5′-CCACATGGAGGGTAAAGTACGGTTAAG-3′) and reverse (5′-CTATTCAGTGGTGGTGGTGGTG-3′) primers, and a synthetic DNA segment encoding the same amino acid sequence but codon-optimized for *Triticum aestivum* (GeneArt AG) was amplified by PCR using the forward 5′-CACTATGGAGGGCAAGGTGCGC-3′ and reverse 5′-GTACTCAGTGGTGATGGTGGTGGTG-3′ primers. The PCR products encoding the native and codon-optimized PfGluRS enzymes were cloned into a cell-free expression vector that carries SP6 RNA polymerase promoter and Ω sequence for the wheat germ ribosome-binding site. *In vitro* transcription and translation were carried out as described (50). PfGluRS was purified from the extracts using Ni-NTA affinity chromatography. Pure fractions observed via SDS-PAGE were pooled, dialyzed against aminoacylation buffer (100 mM Hepes-KOH, pH 7.2, 30 mM KOH, 12 mM $MgCl_2$), and concentrated using Amicon ultracentrifugal filters (Millipore). The yield was 0.75 mg of protein in a total volume of 1 ml.

Expression and Purification of the Mature PfGluRS in Escherichia coli—PfGluRS was also expressed in *E. coli* KRX cells (Promega) containing the pRARE2 plasmid (EMD4BioSciences) and the pET-29a vector encoding the predicted mature PfGluRS coding sequence (Pf3D7_1357200, amino acids 78–574) codon-optimized for *E. coli* (GeneArt, Inc.) with N-terminal His_6 tags. After Ni-NTA chromatography and gel filtration (51), pure fractions were concentrated and dialyzed overnight against aminoacylation buffer containing 0.5 mM DTT and stored at −20 °C in 30% glycerol. The absence of contaminating pyrophosphatase activity was confirmed as described (52).

tRNA Substrates—Synthetic genes encoding *P. falciparum* apicoplast $tRNA^{Glu}$ and $tRNA^{Gln}$ (both from GenBank™ accession number X95276) were prepared by annealing overlapping oligonucleotides, ligated into the pGFIB expression vector (53), and transformed into *E. coli* BL21 cells. Cultures were grown, and crude total tRNA was extracted (54), deacylated in 200 mM Tris-HCl, pH 9, precipitated with isopropyl alcohol, washed with 80% ethanol, air-dried, and resuspended in 500 μl of RNase-free water. Samples were stored at −80 °C until use. Total *E. coli* tRNA (Sigma catalog no. 9014-25-9) was used for the experiment in Fig. 4. The crude *P. falciparum* $tRNA^{Glu}$ and $tRNA^{Gln}$ preparations were each separately ^{32}P-labeled on their 3′ termini using the *E. coli* CCA-adding enzyme and [α-^{32}P]ATP as outlined in Ref. 55.

Aminoacylation Assay and Activation by Pyrophosphatase—The aminoacylation assay using recombinant PfGluRS expressed in *E. coli* was performed and quantified as described in Ref. 55. In experiments testing the effect of PPase, two reactions were initiated simultaneously without PPase and allowed to proceed for 20 min. PPase (10 units/ml) was then added to one reaction and both reactions were incubated for an additional 40 min.

Determination of Kinetic Parameters—The K_m value for L-Glu was determined (55–57) in reactions consisting of varying concentrations of L-Glu (5–400 μM). The K_m values for $tRNA^{Glu}$ and $tRNA^{Gln}$ were determined in varying concentrations of ^{32}P-labeled tRNA (from 0.02 to 5 μM) at an L-Glu concentration of 200 μM. The K_m values for all substrates were determined simultaneously with enzyme aliquots from the same dilution. In all cases the concentration of PfGluRS used was chosen so as to obtain linear kinetics of glutamyl-tRNA formation in a 3-min reaction. Steady-state kinetic parameters were calculated using nonlinear regression based on the Michaelis-Menten equation (GraphPad Prism 5). The aminoacylation discrimination factor D (58) was calculated using the following formula: $D = (k_{cat}/K_m)^{Glu}_{tRNA}/(k_{cat}/K_m)^{Glu}_{tRNA}$.

GluRS Inhibition Assay—The GluRS inhibitor 5′-*O*-[*N*-(L-glutamyl)sulfamoyl]adenosine (Glu-SA) (59) was obtained from IDT (Coralville, IA). To determine the K_i value for Glu-SA inhibition of PfGluRS with respect to L-Glu, we measured the K_m value for L-Glu in the absence of the inhibitor and the K_m^{app} values for L-Glu in the presence of various fixed concentrations of Glu-SA (10 nM to 100 μM). The K_i value was determined from a K_m^{app} *versus* [*I*] plot according to the equation $K_m^{app} = K_m\,(1 + [I]/K_i)$.

Myc Tagging and Attempted Deletion of the Endogenous Plasmodium berghei GluRS Gene—A 4× *myc* tag was appended to the 3′ end of the gene encoding the putative apicoplast-targeted *P. berghei* GluRS (PlasmoDB ID PBANKA_113350) as described (16). A 1.6-kb fragment of the 3′ end of the gene without the stop codon was amplified from *P. berghei* ANKA genomic DNA using primers PbGluRS_F1 (TACCGCGGAAGTGCATATATATGCAAATGCA) and PbGluRS_R (ATACTAGTTATGTTAAATATACTCTTTATGTATTG); the SacII and SpeI restriction sites are underlined. Polymerase chain reactions (PCR) (50 liters) contained 50 ng of genomic DNA, 0.1 μM of each primer, 5 μl of 10× buffer, and 1 μl of Advantage2 polymerase (Clontech). The PCR product was digested with SacII and SpeI and cloned into the b3D *myc* vector (16). *P. berghei* ANKA parasites were transfected, and parasites with *myc* insertions in the GluRS gene were selected and cloned as described (16). Plasmid integration at the 5′ and 3′ insertion sites was confirmed by PCR using primer pairs PbGluRS_For2 (TACCGCGGAAAAGCTTATTATTGCTTTTGCAC) and PbGluRS_int5_Rev2 (GAGACAGCTCAATTCTTTATGTCC) for the 5′ integration test, and PbGluRS_int3_For2 (CCTCTTCGCTATTACGCCAGCT) and PbGluRS_int3_Rev2 (GTGAAATACGAGTATTAATATACAGG) for the 3′ integration test.

The strategy described previously (60) was used to attempt deletion of the *PbGluRS* gene by double crossover recombination. The primers used to amplify the genomic regions were as follows: PbGluRS_apico_KO.Pr1For (GCCCGCGGAATTTATTGAAAATATGGTTATCAGC); PbGluRS_apico_KO.Pr2Rev (TCATACTGTGGGCCCATAGAAGGAATTACACATAACAAGG); PbGluRS_apico_KO.Pr3For, TCCTTCTATGGGCCCACAGTATGAATTAAATTTGGTCAC); and PbGluRS_apico_KO.Pr4Rev (GCGCGGCCGCTTACTTTGTGATTCAGTTGCGC). Primers 1 and 2 were designed to amplify a 952-bp fragment containing the last 102 bp of the *PbGluRS* coding sequence and 850 bp of the 3′ UTR. Primers 3 and 4 were designed to amplify an 813-nucleotide fragment containing the first 62 bp of the *PbGluRS* coding sequence and 751 bp of the 5′ UTR. Primer 1 contained an added 5′-terminal GC dinucleotide and a SacII site. Primer 4 contained an added 5′-terminal GC dinucleotide and a NotI site. Primers 2 and 3 contained an ApaI site flanked by complementary sequences (underlined) for recombinatorial PCR. The two genomic fragments were first amplified in separate reactions using the cycling parameters described above, and the resulting products were combined in a second PCR to form a single product, which was digested with SacII and NotI and cloned into the B3D KO Red vector. This construct was linearized with ApaI, and *P. berghei* ANKA parasites were transfected as described (61). Pyrimethamine-resistant parasites were genotyped by PCR using the following primer pairs: ORF test, PbGluRS_For1 and PbGluRS_Rev; Test 1 For (ATATTCTGCGATTTTTCTTG) and Test 1 Rev (GCAAGGCGATTAAGTTGGGT); Test 2 For (GGCTACGTCCCGCACGGACGAATCCAGATGG) and Test 2 Rev (AGTATAACACTCTCTATCCTAAAA).

Subcellular Localization—Analysis of the *P. berghei* clones expressing Myc-tagged PbGluRS was performed as outlined in Ref. 62. Double staining was performed using a rabbit polyclonal

anti-acyl carrier protein (ACP) primary antibody (diluted 1:500) (63) as an apicoplast marker and mouse monoclonal anti-Myc antibody (Santa Cruz Biotechnology, diluted 1:500) to detect PbGluRS-myc. Fluorescent staining was achieved with Alexa Fluor-conjugated secondary antibodies (Invitrogen) specific to rabbit (Alexa Fluor 594, red) and mouse (Alexa Fluor 488, green) IgG. DAPI was used to stain nucleic acids, and the mitochondrion was stained by incubating the parasites in culture media for 30 min with 20 nM MitoTracker Red (Invitrogen), and fixing the cells as outlined above. Images were acquired using an Olympus Delta Vision imaging system (Applied Precision) with a ×100 objective and deconvolved using the Softworx package (Applied Precision) with the default parameters.

RESULTS

Components of the Apicoplast Indirect Aminoacylation Pathway—The first step in the indirect aminoacylation pathway for Gln-tRNA^{Gln} biosynthesis is glutamylation of tRNA^{Gln} by a nondiscriminating GluRS. The *P. falciparum* genome (10) encodes two putative GluRS enzymes, one of which (Pf3D7_1357200, 68.4 kDa, 574 amino acids) possesses a predicted N-terminal apicoplast-targeting sequence (64, 65). The other, Pf3D7_1349200, appears to be cytoplasmic (66), suggesting that the enzyme encoded by Pf3D7_1357200 is the apicoplast GluRS and therefore should possess nondiscriminating activity. Apicoplast-targeted PfGluRS orthologs are present in all sequenced plasmodia, *Theileria* and *Toxoplasma,* but not in apicomplexans that lack apicoplasts. Organisms, or organelles, that utilize the indirect aminoacylation pathway for Gln-tRNA^{Gln} biosynthesis often, but not always (67), lack GlnRS. Consistent with this, malaria parasites possess only one GlnRS (Pf3D7_1331700) that lacks an apicoplast targeting signal and is probably cytoplasmic (66, 68). Nuclear genes encoding apicoplast-targeted *P. falciparum* orthologs of the GatA and GatB subunits of bacterial Glu-AdT were also identified, but not GatC.[5] GatC is a small, poorly conserved protein (12 kDa) that appears to perform a purely structural role at the interface between the GatA and GatB subunits in bacterial Glu-AdTs (69). A potential *Plasmodium* GatC ortholog may be difficult to detect by similarity searches. Furthermore, we did not find a *Plasmodium* ortholog of the GatF subunit of yeast mitochondrial Glu-AdT (70). Finally, putative tRNA^{Glu} and tRNA^{Gln} substrates of GluRS and Glu-AdT are encoded by the apicoplast genome (5). Thus, except for an ortholog of GatC, we identified all components of the indirect aminoacylation pathway in *P. falciparum* (Table 1) and in other apicoplast-containing apicomplexan parasites.

Isolation of the PfGluRS cDNA from Blood Stages—The predicted Pf3D7_1357200 gene encoding PfGluRS contained seven exons, but the gene structure had not yet been confirmed experimentally. We isolated a RT-PCR product from *P. falciparum* blood stage total RNA that confirmed the annotated gene structure. Microarray-based gene expression analyses also showed that the PfGluRS gene was transcribed in asexual parasites, with moderate induction in late trophozoites, and that its expression occurred in-phase with genes transcribed from the apicoplast genome (71). PfGluRS transcripts were identified in blood stage parasites using RNA-Seq (72), and the protein was also detected in gametocytes via proteomics (73, 74).

TABLE 1
Components of the apicoplast indirect aminoacylation pathway in *P. falciparum* and *P. berghei*
PlasmoDB identifiers for the nucleus-encoded proteins are indicated.

Component	*P. falciparum*	*P. berghei*
GluRS	PF3D7_1357200	PBANKA_113350
Glu-AdT GatA subunit	PF3D7_0416100	PBANKA_071810
Glu-AdT GatB subunit	PF3D7_0628800	PBANKA_112750
tRNA^{Glu}	Apicoplast[a]	Apicoplast[b]
tRNA^{Gln}	Apicoplast[a]	Apicoplast[b]

[a] GenBank™ accession number X95276 (5) was used.
[b] The *P. berghei* apicoplast genome sequence was obtained from the Wellcome Trust Sanger Institute FTP site.

Sequence Comparison of the PfGluRS and Bacterial Orthologs—Aminoacyl tRNA synthetases are classified into two major groups. Class I enzymes contain an N-terminal catalytic domain and generally acylate the 2′-hydroxyl of the terminal tRNA adenosine, whereas the catalytic domains of class II enzymes possess a seven-stranded anti-parallel β-sheet fold flanked by α-helices and acylate the 3′-hydroxyl of the tRNA adenosine. Glutamyl-tRNA synthetases are class I enzymes (75). The PfGluRS amino acid sequence was aligned with those of several prokaryotic orthologs (Fig. 1) to identify conserved and divergent features. The PfGluRS possesses the "HIGH" and "KMSKF" ATP-binding motifs that are characteristic of the Rossman fold (75). Other features common to class I GluRSs that were well conserved in PfGluRS included residues that interact with the L-glutamate, ATP, and tRNA^{Glu} substrates (76). A zinc-binding SWIM motif ($CXCX_{24}CX_{24}H$; *open circles* in Fig. 1) in the *E. coli* GluRS is essential for catalytic activity (77) but is not completely conserved in the PfGluRS ($CXCX_{24}CX_{24}D$). The His residue in the bacterial SWIM motif is required for Zn^{2+} binding but is replaced in PfGluRS by an Asp residue, which is a potential Zn^{2+} ligand. Other GluRSs also lack a canonical SWIM motif and do not bind or require Zn^{2+} for activity (78). We found that PfGluRS did not require Zn^{2+} supplementation for *in vitro* activity, and the ZincPred server (79) did not identify any zinc-binding sites in the protein. Finally, the *Plasmodium* enzyme has an N-terminal extension, the bipartite apicoplast-targeting signal, that prokaryotic enzymes lack (64, 65).

Nondiscriminating GluRSs differ from discriminating enzymes in that they can glutamylate the cognate substrate tRNA^{Glu} as well as the noncognate substrate tRNA^{Gln}. Recognition and discrimination of tRNA substrates by GluRS (78, 80) requires that the enzyme is able to distinguish between the tRNA^{Glu} UUC and tRNA^{Gln} UUG anticodons. The alignment (Fig. 1) revealed similarities between the PfGluRS and nondiscriminating bacterial and cyanobacterial enzymes at two residues critical for tRNA anticodon discrimination. The thermophilic eubacterium *Thermus thermophilus* possesses a single discriminating GluRS (81). Structural analysis of the *T. thermophilus* GluRS revealed that the bulky side chain of the Arg-358 residue in the anticodon binding pocket (position 442 in Fig. 1) recognizes the pyrimidine base of C36 in the anticodon of the tRNA^{Glu} substrate. However, in the cyanobacterium *Thermosynechococcus elongatus*, which has a single nondiscriminating GluRS, Arg-

[5] M. J. Gardner and B. M. Mailu, unpublished observations.

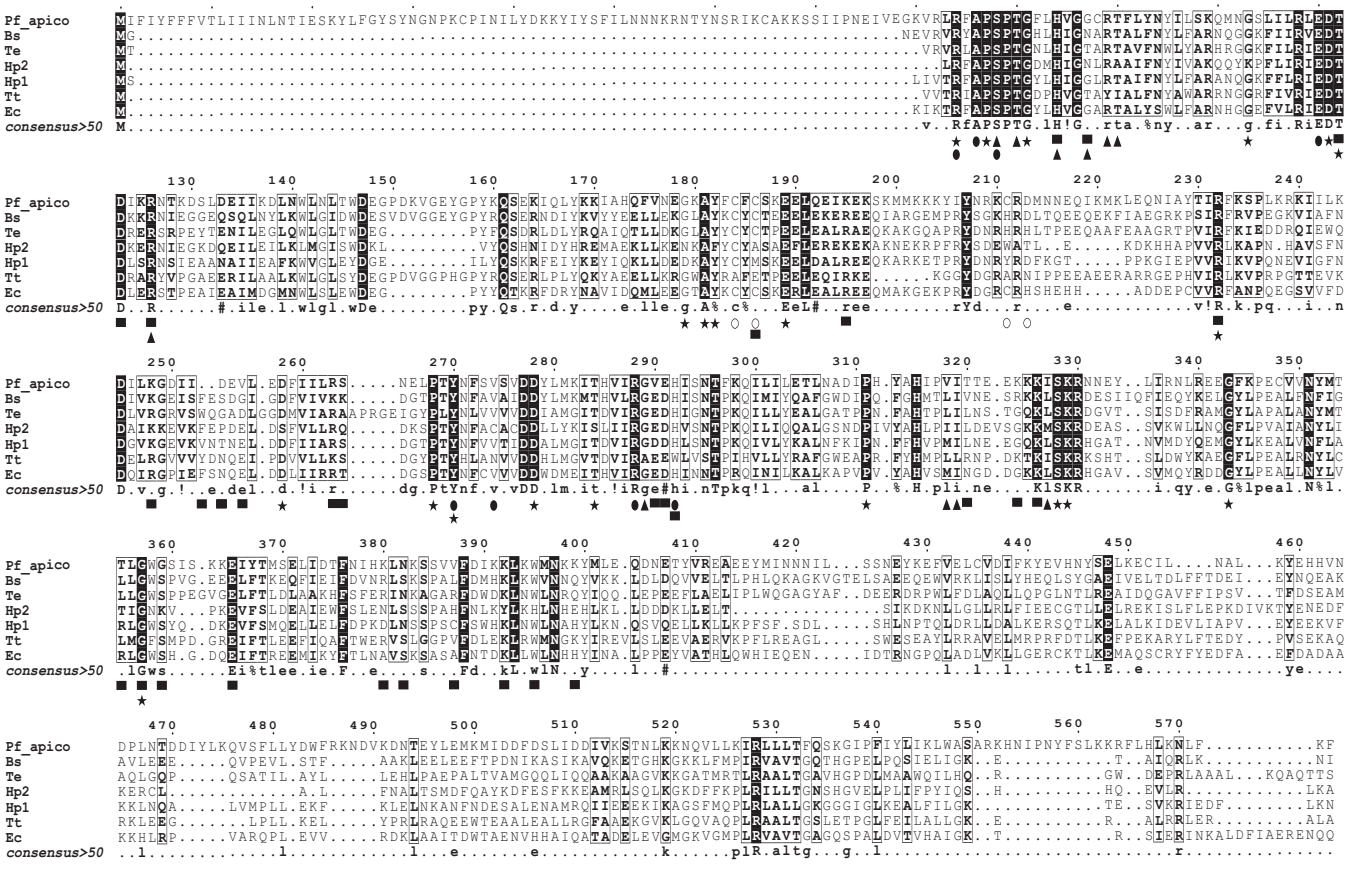

FIGURE 1. **Alignment of the *P. falciparum* apicoplast PfGluRS amino acid sequence with bacterial orthologs.** The PfGluRS amino acid sequence was aligned with those of bacterial and cyanobacterial orthologs using tCoffee-Expresso (42). Sequences and UniProt accessions are as follows: *Pf_apico*, *P. falciparum* apicoplast GluRS (Q8IDD3); *Bs*, *Bacillus subtilis* (P22250); *Te*, *Thermosynechococcus elongatus* (Q8DLI5); *Hp1*, *Helicobacter pylori* GluRS1 (P96551); *Hp2*, *H. pylori* GluRS2 (O25360); *Tt*, *T. thermophilus* (P27000); *Ec*, *E. coli* (P04805). Residues are highlighted as follows (76): residues conserved in the GluRS/GlnRS family, *stars*; interactions with L-glutamate, *solid circles*; productive interactions with ATP, *solid triangles*; interactions with tRNA substrate, *solid black squares*. The *open circles* indicate the zinc-binding residues identified in the *E. coli* GluRS (107). Residues 94–94 and 326–330 correspond to the HIGH and "KMSKF" ATP-binding motifs of class I aaRSs (75). The N-terminal extension (*gray highlighting*) in the PfGluRS sequence is the bipartite apicoplast targeting sequence.

358 is replaced by an uncharged Gly residue. The smaller Gly side chain forms a larger pocket that allows recognition of the purine base of G36 in the noncognate $tRNA^{Gln}$ as well as the $tRNA^{Glu}$ C36 nucleotide in the cognate $tRNA^{Glu}$ (78). Six other amino acid substitutions of this Arg residue (Gln, Ser, Glu, Asn, Tyr, and His) have been observed in other nondiscriminating GluRSs (80). A second residue involved in anticodon discrimination is Thr-444 in the *T. thermophilus* GluRS (position 537 in Fig. 1), which is substituted by Gly in *T. elongatus* and most other nondiscriminating GluRSs (80). The PfGluRS contains Glu and Gly at these positions, respectively, which is consistent with other nondiscriminating GluRSs and our analyses of PfGluRS aminoacylation activity (see below).

Phylogenetic Analysis—A maximum likelihood phylogenetic tree was constructed of the apicoplast PfGluRS, the human and *P. falciparum* cytoplasmic GluRSs, and GluRSs from several bacteria and an archaeon. As shown in Fig. 2, PfGluRS resolved with bacterial enzymes, consistent with an organellar origin, and not with eukaryotic cytoplasmic or archaeal enzymes.

Expression of Recombinant PfGluRS in Wheat Germ Extracts and E. coli—We used the multiple sequence alignment of PfGluRS and bacterial orthologs (Fig. 1) and predictions from

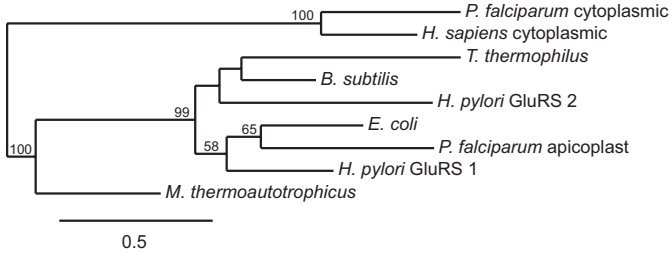

FIGURE 2. **Phylogenetic analysis of the apicoplast PfGluRS and archaeal, bacterial, and eukaryotic orthologs.** A maximum likelihood tree of representative GluRS sequences from the three domains of life. *Scale bar,* 0.5 changes/site.

PlasmoAP (65) and PATS (64) to estimate the N-terminal residue of the mature PfGluRS. Residue Glu-78 was selected because it is N-terminal to the conserved ATP-binding site and within the N-terminal extension of the PfGluRS. Initial attempts to express PfGluRS in *E. coli* were not successful, but a wheat germ system was used to first validate that the gene coded for the aminoacylation activity. Wheat germ extracts had been used previously to express catalytically active *P. falciparum* dihydrofolate reductase (DHFR-TS) (50). Recombinant PfGluRS was expressed in the extracts at a level similar to that

observed with PfDHFR-TS. Furthermore, the PfGluRS produced in wheat germ could glutamylate apicoplast $tRNA^{Glu}$, an activity that was not present in control extracts that expressed green fluorescent protein (GFP), suggesting that the *Plasmodium* enzyme was functional.[5] In an attempt to increase the yield, we subsequently expressed a codon-optimized version (for wheat) of the PfGluRS coding sequence in extracts, and we included [^{14}C]Leu to detect newly synthesized proteins. Codon optimization dramatically increased the amount of PfGluRS produced in comparison with the same protein encoded by the native sequence. This is clearly evident in an SDS-polyacrylamide gel stained with Coomassie Blue (Fig. 3*A*) and autoradiographed (Fig. 3*B*). Most of the ^{14}C-labeled protein in extracts that expressed the wild-type PfGluRS migrated at 32 kDa, about half of the predicted size, whereas virtually all of the ^{14}C-labeled protein in extracts expressing the codon-optimized version appeared to be full length. PfGluRS produced using the codon-optimized construct also possessed glutamylation activity.[5] We therefore applied the same codon optimization strategy to express PfGluRS in *E. coli*, and we purified the enzyme via Ni-NTA and gel filtration chromatography. SDS-PAGE revealed a single band of ~63 kDa (Fig. 4*A*) that reacted with anti-His antibody in a Western blot. However, a faster migrating band formed upon storage and the specific activity of the enzyme declined, indicating that PfGluRS was susceptible to oxidation. Consequently, DTT was included in both storage and reaction buffers, which prevented formation of the faster migrating band and preserved enzyme activity. We routinely obtained 20 mg of pure enzyme/liter of culture. PfGluRS produced in *E. coli* was used for the enzyme kinetics and inhibition assays.

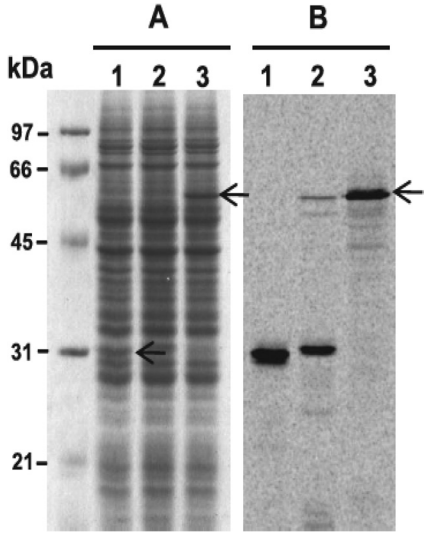

FIGURE 3. **Analysis of PfGluRS and GFP expressed in wheat germ extracts.** *A,* Coomassie-stained SDS-polyacrylamide gel of soluble proteins in wheat germ extracts expressing GFP or PfGluRS in the presence of [^{14}C]leucine. *Lane 1,* GFP; *lane 2,* native (*wild type*) PfGluRS; *lane 3,* codon-optimized PfGluRS. *B,* autoradiograph of the gel in *A*.

PfGluRS Is a Nondiscriminating Enzyme—We hypothesized that the PfGluRS encoded by Pf3D7_1357200 was the first of two enzymes in an indirect aminoacylation pathway. As such, it should possess nondiscriminating activity and glutamylate apicoplast $tRNA^{Gln}$ as well as $tRNA^{Glu}$. To test this hypothesis, aminoacylation assays were performed with mature PfGluRS in the presence of either apicoplast $tRNA^{Glu}$ or $tRNA^{Gln}$ substrates (52, 82). Briefly, crude preparations of each apicoplast tRNA expressed in *E. coli* were ^{32}P-labeled at their 3′-terminal AMP with [α-^{32}P]AMP using the nucleotide exchange activity of *E. coli* CCA-adding enzyme. The labeled tRNAs were then incubated with recombinant PfGluRS, and at various time points an aliquot of the reaction was withdrawn and added to an acidic solution of nuclease P1 to simultaneously quench the reaction, prevent deacylation, and digest the tRNA to mononucleotides. Next, the reaction products were subjected to TLC to sep-

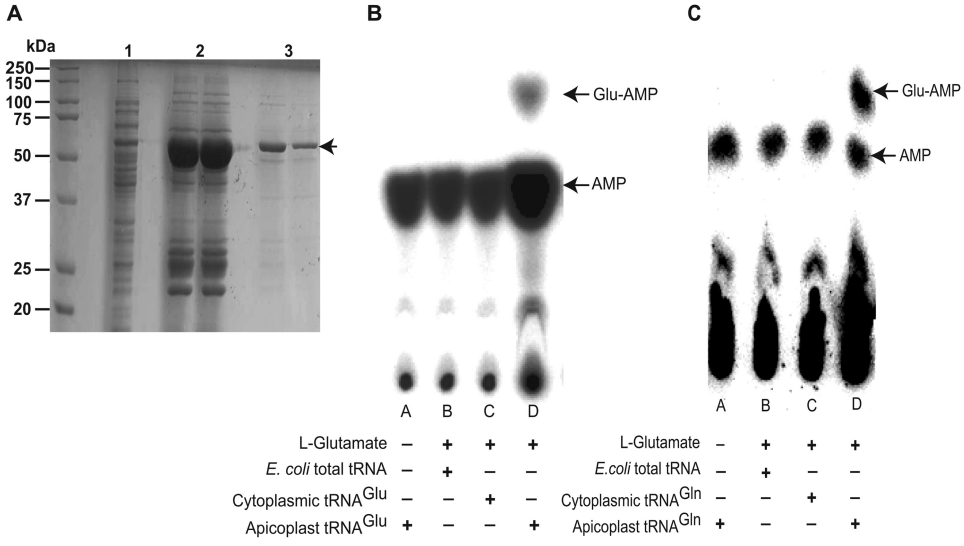

FIGURE 4. **Mature apicoplast PfGluRS purification and aminoacylation assay.** *A,* purification of the mature PfGluRS assessed by 7.5% SDS-PAGE. *Lane 1,* crude *E. coli* lysate; *lane 2,* eluate from an Ni-NTA column; *lane 3,* eluate from gel filtration purification. *B* and *C,* representative phosphorimages of the separation of Glu-[α-^{32}P]AMP and [α-^{32}P]AMP by PEI-cellulose TLC after PfGluRS-catalyzed aminoacylation. The aminoacylation assays were performed as described under "Experimental Procedures" with the following modifications. *B,* reactions in *lanes A* and *D* contained apicoplast $tRNA^{Glu}$, but L-glutamate was omitted from *lane A*. *Lane B* contained *E. coli* tRNA, and *lane C* contained *Pf* cytoplasmic $tRNA^{Glu}$. *C,* reactions in *lanes A* and *D* contained apicoplast $tRNA^{Gln}$ but L-glutamate was omitted from *lane A*. *Lane B* contained *E. coli* tRNA and *lane C* contained *P. falciparum* cytoplasmic $tRNA^{Gln}$. Apicoplast PfGluRS is a nondiscriminating enzyme that is capable of specifically glutamylating both of the apicoplast tRNA substrates.

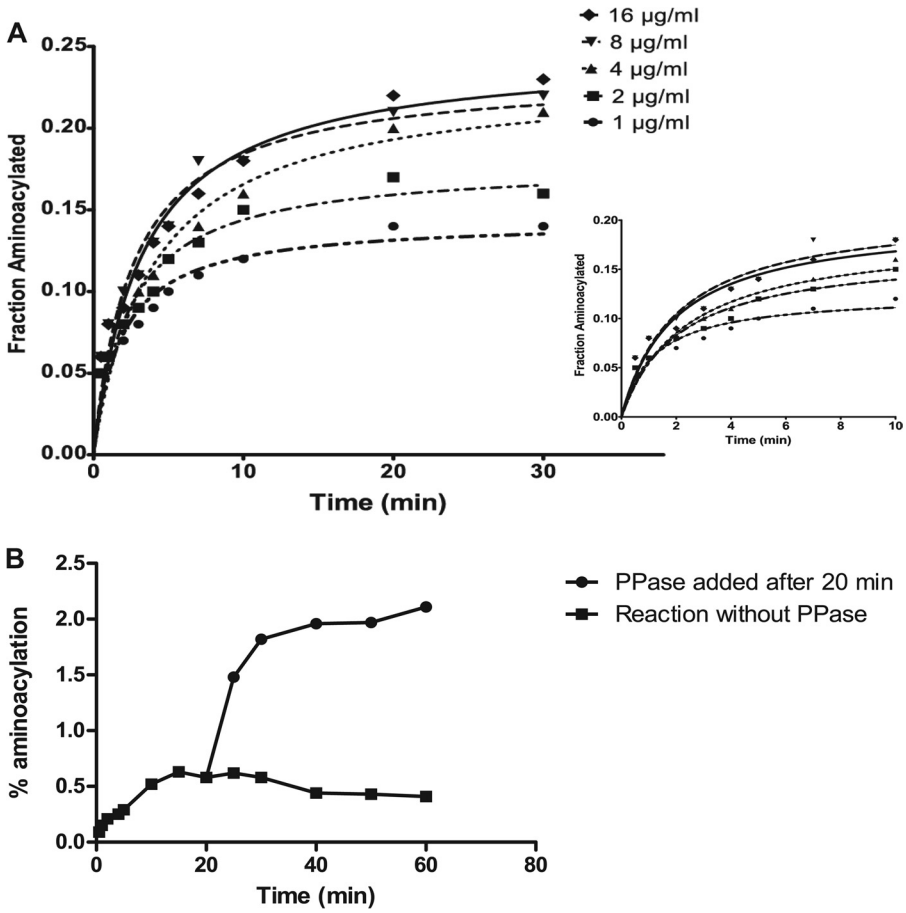

FIGURE 5. **PfGluRS aminoacylation time course assays and stimulation of activity by pyrophosphatase.** *A,* normalized plot of tRNA^{Glu} aminoacylation time course assays performed using the indicated concentrations of PfGluRS. *Inset,* enlarged view of the period between 0 and 10 min. *B,* two aminoacylation assays containing 4 μg/ml of PfGluRS were initiated simultaneously and allowed to proceed for 20 min in the absence of PPase. After 20 min, PPase (10 units/ml) was added to one reaction, and both reactions were incubated for an additional 40 min.

arate [^{32}P]AMP from glutamyl-[^{32}P]AMP, and the extent of aminoacylation was calculated from the ratio of the radioactivity of the two spots as determined by phosphorimaging. As shown in Fig. 4, *B* and *C*, both of the apicoplast tRNA substrates were glutamylated, demonstrating that the PfGluRS is a nondiscriminating enzyme. PfGluRS did not utilize L-glutamine as a substrate[5] and did not glutamylate cytoplasmic *P. falciparum* tRNA^{Glu} and tRNA^{Gln} or *E. coli* tRNA (Fig. 4, *B* and *C*). Because nondiscriminating GluRSs are often found in cells or organelles that lack GlnRS and must use indirect aminoacylation for Gln-tRNA^{Gln} biosynthesis, this finding provides strong biochemical evidence that the indirect pathway is used in the *Plasmodium* apicoplast.

Effect of PPase on PfGluRS Aminoacylation Activity—Aminoacylation reactions performed with varying amounts of PfGluRS clearly showed that an increase in enzyme concentration was accompanied by an increase in the reaction rate (Fig. 5*A*). However, the aminoacylation activity plateaued within a few minutes after enzyme addition, an effect suggestive of product inhibition. Adding more PfGluRS to the reaction after it had plateaued did not increase aminoacylation, implying that this effect was not an artifact caused by enzyme denaturation. Because inorganic pyrophosphate (PP_i) can inhibit tRNA synthetase activity (52), we added PPase to an aminoacylation assay after the reaction had plateaued. This dramatically stimulated the PfGluRS reaction rate and increased the steady-state level of the Glu-tRNA^{Glu} product ~3-fold compared with reactions without PPase (Fig. 5*B*). Enhanced PfGluRS activity in the presence of PPase indicated that the strong inhibition observed in its absence was due to the generation of PP_i during the reaction.

TABLE 2
Kinetic analyses of PfGluRS

The K_m value for the tRNA substrates was determined in reactions containing 100 mM Hepes-KOH, pH 7.2, 30 mM KOH, 12 mM $MgCl_2$, 2 mM DTT, 4 mM ATP, 200 μM L-glutamate, 4 μg/ml recombinant PfGluRS expressed in *E. coli* and varying concentrations of the indicated ^{32}P-labeled tRNA from 0.02 to 5 μM. NA means not applicable.

Substrate	PPase	K_m	k_{cat}	k_{cat}/K_m	D-factor[a]
		μM	s^{-1}	$s^{-1}\ \mu M^{-1}$	
tRNA^{Glu}	−	0.0497 ± 0.0097	0.43 ± 0.027	8.65	1.59
tRNA^{Gln}	−	0.0767 ± 0.0031	0.42 ± 0.047	5.43	
tRNA^{Glu}	+	0.0032 ± 0.0007	3.61 ± 1.15	112.67	4.86
tRNA^{Gln}	+	0.0911 ± 0.0054	2.11 ± 1.58	23.17	
L-Glu	−	1.401 ± 0.61	1.39 ± 0.098	0.99	NA
ATP	−	2.35 ± 0.67	1.18 ± 0.307	0.704	NA

[a] D-factor = $(k_{cat}/K_m\ tRNA^{Glu})/(k_{cat}/K_m\ tRNA^{Gln})$.

Kinetic Analyses—Having demonstrated PfGluRS aminoacylation activity and inhibition by PP_i, we next conducted kinetic analyses to determine optimal reaction parameters and to compare the *Plasmodium* enzyme to bacterial orthologs. PfGluRS demonstrated higher affinities toward the cognate as compared with the noncognate tRNA substrate (Table 2). We then determined the same kinetic values for PfGluRS in reactions contain-

ing PPase. Here, the stimulatory effect of PPase was dramatic, increasing turnover by 8.4- and 5-fold and catalytic efficiency by 13- and 4-fold, for $tRNA^{Glu}$ and $tRNA^{Gln}$ substrates, respectively, in comparison with reactions performed in its absence. The discrimination factor, *D*, a measure that compares enzyme turnover rates for cognate and noncognate substrates at the same concentration (83) was also calculated, revealing that PfGluRS glutamylated the cognate $tRNA^{Glu}$ substrate more efficiently than the noncognate $tRNA^{Gln}$ substrate, an effect that was most pronounced in the presence of PPase.

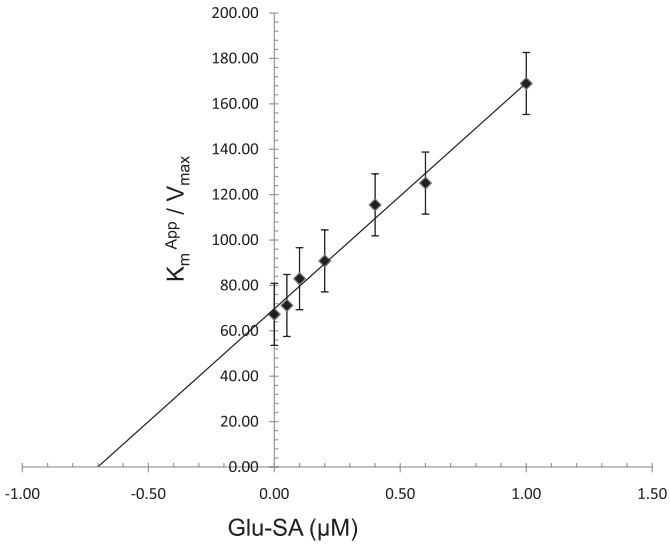

FIGURE 6. **Competitive inhibition of PfGluRS by Glu-SA.** The K_m^{app} for glutamate was determined with 400 μM L-glutamate in the presence of 0–1 μM Glu-SA at 37 °C. The data show that Glu-SA is a competitive inhibitor of PfGluRS with respect to L-glutamate with a K_i of 0.7 μM.

PfGluRS Inhibition by a Bacterial GluRS Inhibitor—Glu-SA, a GluRS inhibitor, is a stable analog of the glutamyl-AMP intermediate of the aminoacylation reaction (59). It belongs to a group of synthetic aminoacyl adenylates called aminoacylsulfamoyladenosines in which the labile mixed anhydride function of the aminoacyladenylate intermediate in the aminoacylation reaction is replaced by an isosteric, nonhydrolyzable sulfamoyl group (84). Glu-SA is a strong competitive inhibitor of the *E. coli* GluRS (K_i = 2.8 nM) but is a weaker competitive inhibitor of mammalian (mouse liver) GluRS (K_i = 70 nM) (59). Using the aminoacylation assay employed above to determine the kinetic values for PfGluRS, we found that Glu-SA is a competitive inhibitor of the mature PfGluRS (Fig. 6). However, Glu-SA is much less potent against the *P. falciparum* enzyme (K_i = 0.7 μM) than it is against either the *E. coli* or mammalian GluRSs.

Subcellular Localization—The *P. falciparum* GluRS encoded by Pf3D7_1357200 contains a predicted apicoplast targeting sequence (10, 65, 85), but the subcellular localization of the enzyme has never been established experimentally. To determine whether the enzyme is targeted to the apicoplast *in vivo*, we tagged the endogenous gene encoding the *P. berghei* ortholog of PfGluRS (Table 1) with a quadruple Myc tag (Fig. 7). We tagged the endogenous *PbGluRS* coding sequence so that the native promoter controlled the timing and level of expression, minimizing the possibility that the fusion protein would

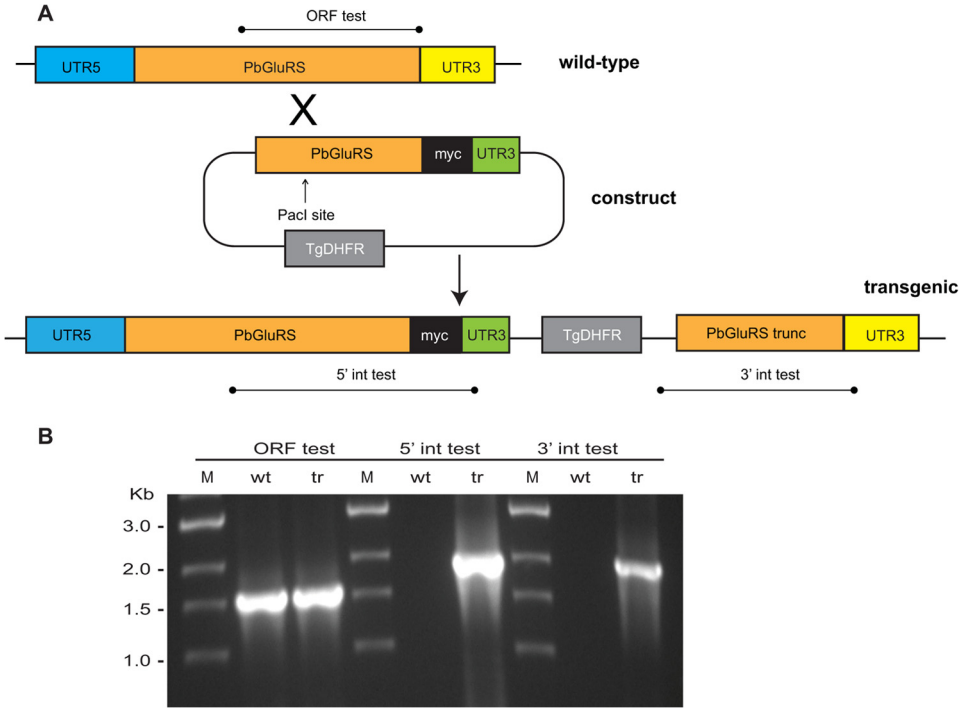

FIGURE 7. **Integration of a second copy of GluRS fused to a quadruple Myc tag (PbGluRS-myc) into the *P. berghei* genome.** *A,* 1.6-kb fragment of the 3′ end of the GluRS gene without the stop codon was amplified from *P. berghei* ANKA genomic DNA and ligated upstream of the quadruple Myc tag in the b3D myc vector (16). Following linearization of the construct with PacI, it was transfected into *P. berghei* blood stage schizonts that were subsequently injected into mice. The vector contains a mutated *T. gondii DHFR/TS* gene as a pyrimethamine selectable marker (*TgDHFR*), and transgenic parasites were selected by pyrimethamine treatment and cloned by limiting dilution. *B,* PCR analysis of the integration site in a cloned PbGluRS-*myc* transgenic (*tr*) parasite. Ethidium bromide-stained agarose gels showing the integration of the PbGluRS-myc vector into the *P. berghei* genome. Only PbGluRS-*myc* is positive in the 3′ and 5′ integration (*int*) tests, whereas both PbGluRS-*myc* and wild-type (*wt*) parasite genomic DNAs are positive for the PbGluRS open reading frame test (ORF test). *M* indicates the size ladder.

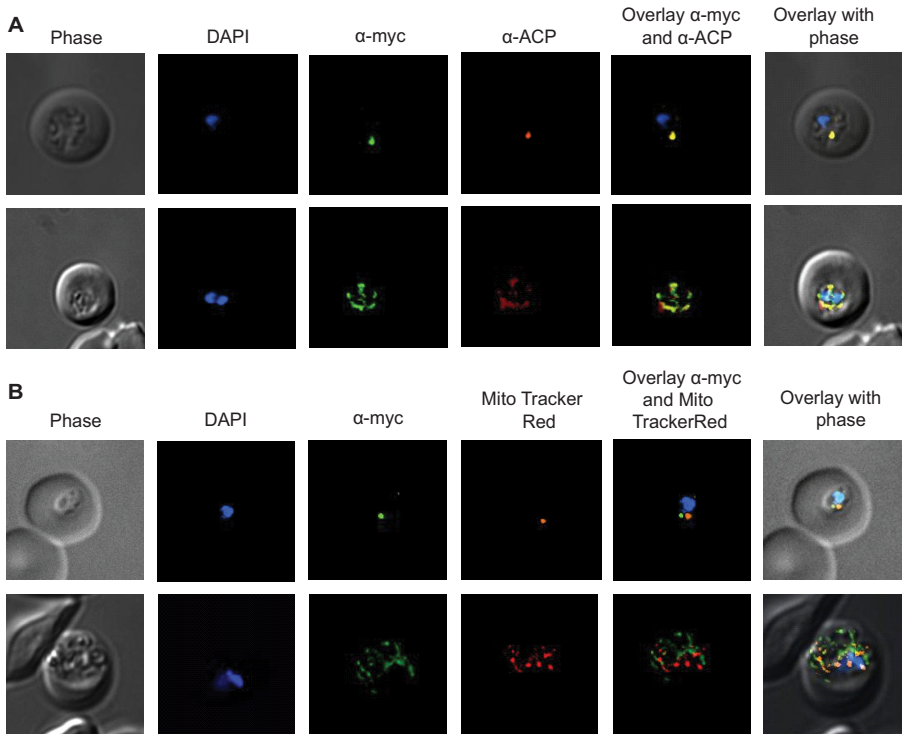

FIGURE 8. **PbGluRS localizes to the apicoplast.** Transgenic *PbGluRS-myc* parasites were generated in which the protein was expressed under the control of the endogenous promoter with a C-terminal quadruple Myc tag. Differential interference contrast and fluorescent images were captured and processed using deconvolution microscopy; a merge of the images is presented on the *far right column* (*overlay*). *A,* PbGluRS-Myc apicoplast localization was monitored by immunofluorescence assay using an anti-Myc antibody (*green*), and the apicoplast was detected by staining with anti-ACP antibody (*red*). Nucleic acid was stained with DAPI (*blue*). PbGluRS-Myc marks a characteristically small and round compartment early in the infection cycle (*top row*), which then elongates and develops into a complex, multiply branched form at the trophozoite stage prior to splitting into individual spots, one for each merozoite, in the schizont stage (*bottom row*). PbGluRS-Myc co-localized with ACP (*α-Myc/α-ACP overlay*) confirming localization to the plastid. *B*, PbGluRS is not localized to the mitochondrion in erythrocytic stages. The mitochondrion was labeled using MitoTracker Red, and PbGluRS-Myc was detected by immunofluorescence assay using an anti-Myc antibody (*green*). Nucleic acid was stained with DAPI. In the early stages of parasite development (*top row*), PbGluRS-Myc and the mitochondria are discrete single organelles. In the late trophozoite stages, the mitochondria and PbGluRS-Myc are heavily branched but mostly distinct with a few points of overlapping signal (*bottom row*). In late schizonts, PbGluRS-Myc and mitochondria form single organelles. *Scale bar,* 1 μm.

be mis-targeted. Fixed blood stage parasites were stained with anti-Myc antibody to detect PbGluRS and ACP antisera (9) to detect the apicoplast, and the samples were observed using Deltavision deconvolution fluorescence microscopy. Structures containing the Myc-tagged PbGluRS (PbGluRS-myc) exhibited a typical apicoplast appearance (Fig. 8*A*). PbGluRS-Myc marked a small spherical compartment in ring stage parasites (Fig. 8*A*), which then elongated and developed into a complex branched form at the trophozoite stage (Fig. 8*A*) prior to splitting into numerous individual structures in schizonts, one for each daughter merozoite. PbGluRS-Myc co-localized with ACP (Fig. 8*A, α-Myc/α-ACP overlay*), confirming that it is targeted to the apicoplast. This result demonstrated that the *PbGluRS* genomic locus is susceptible to integration of plasmid DNA.

To investigate potential localization to the mitochondrion, live parasites expressing PbGluRS-myc were incubated with MitoTracker Red and then fixed, stained with anti-Myc monoclonal antibody, and examined by fluorescence microscopy. In ring stages, the anti-Myc antibody and MitoTracker Red marked distinct organelles that were closely apposed to each other (Fig. 8*B*). Little co-localization between the mitochondrion and PbGluRS-Myc was observed in late trophozoites or early schizont stages with the mitochondrial staining largely distinct from that of PbGluRS-Myc, apart from a few apparent points of contact between the two organelles (Fig. 8*B*). Close apposition of the mitochondrion and apicoplast has been previously observed in *Plasmodium* spp. (86). At the late schizont stage, the mitochondria and the apicoplast again appeared as closely apposed but distinct organelles adjacent to the nuclei. Together with our demonstration above that PbGluRS co-localizes with the apicoplast protein ACP (Fig. 8*A*), these observations show that PbGluRS-myc is located within the apicoplast but not the mitochondrion in erythrocytic parasites. Finally, a bipartite apicoplast-targeting sequence from a *Babesia bovis* GluRS was recently shown (87) to direct GFP into the *Babesia* apicoplast. This is consistent with our localization of the PfGluRS by an analogous approach,[5] and by epitope tagging of the endogenous PbGluRS enzyme (Figs. 8 and 9).

Attempted Deletion of the PbGluRS Gene—The apicoplast GluRS should be essential because it produces two substrates for apicoplast protein synthesis, Glu-tRNA^{Glu} directly, and Gln-tRNA^{Gln} indirectly, in concert with a Glu-AdT. Because bioinformatic analyses suggest that *Plasmodium* lacks an apicoplast-targeted GlnRS (66, 88), indirect aminoacylation is probably the sole route for Gln-tRNA^{Gln} formation in the apicoplast. To test whether PbGluRS was required for blood-stage growth, we transfected *P. berghei* parasites with a construct (Fig. 9) designed to delete the endogenous *PbGluRS* gene by double crossover recombination. As a control, we transfected parasites from the same batch with the same construct (Fig. 7)

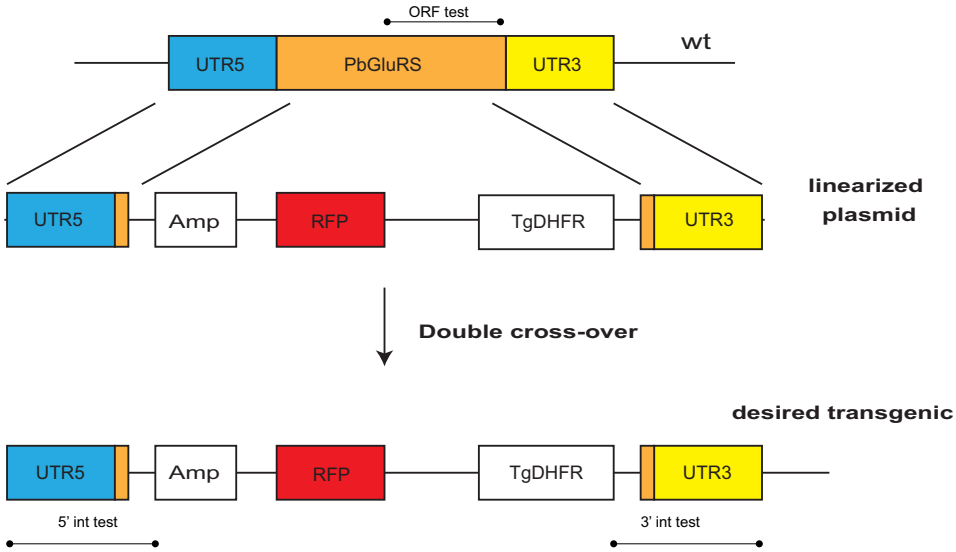

FIGURE 9. **Attempted knock-out of the *PbGluRS* gene by double crossover recombination (replacement).** Two fragments containing 5′- and 3′-UTRs of the *PbGluRS* gene, with ~100 nucleotides of the start and end, respectively, of the *PbGluRS* coding sequence were cloned into the B3D KO Red vector (60). After linearization with ApaI, the construct was transfected into *P. berghei* ANKA parasites (108). In three independent experiments, we were unable to delete the endogenous *PbGluRS* gene by integration of the deletion construct via double crossover recombination.

used to generate the *PbGluRSmyc* transgenic parasites. In three independent experiments, we were unable to integrate the deletion construct into the *PbGluRS* genomic locus via double crossover recombination. As shown earlier, however, transgenic *PbGluRSmyc* parasites were readily obtained (data not shown). These results indicate that the *PbGluRS* locus was accessible to recombination but that the gene could not be deleted, strongly suggesting that the apicoplast-targeted GluRS is essential in blood stage parasites.

DISCUSSION

Plasmodium aaRSs have not been widely studied despite their critical role in protein synthesis, a process absolutely required for parasite replication. One early study reported aaRS activity in *P. berghei* cell-free extracts (89), and genome sequencing later revealed the entire complement of aaRSs in *Plasmodium* (10, 68, 88). But to date, cytoplasmic and apicoplast *P. falciparum* aspartyl-tRNA synthetase (28, 29), lysyl-tRNA synthetase (30, 31), and tryptophanyl-tRNA synthetase (32, 33) are the only other malarial aaRSs besides PfGluRS to be functionally or structurally characterized.

To our knowledge, the apicoplast PfGluRS is only the second apicoplast aaRS to be biochemically characterized. Recently, aminoacylation by recombinant apicoplast LysRS (PF3D7_1416800) was shown to be inhibited by a series of novel compounds that mimicked the lysyl-adenylate reaction intermediate, and two compounds exhibited IC_{50} values in the 40–85 nM range against asexual parasites i*n vitro* (28). Istvan *et al.* (90) also showed that apicoplast isoleucyl-tRNA synthetase (PF3D7_1225100) is the target of mupirocin, an inhibitor of bacterial isoleucyl-tRNA synthetases used to treat skin infections. Mupirocin also inhibited parasite growth *in vitro* at very low concentrations (EC_{50} ~58 nM). Together, these results suggest that inhibitors of other apicoplast aaRSs might also exhibit good anti-parasitic activity (91).

We used recombinant PfGluRS produced in *E. coli* (Fig. 3) to conduct biochemical analyses to determine whether the enzyme had nondiscriminating aminoacylation activity required for indirect aminoacylation and to establish optimal reaction conditions. We chose to use an aminoacylation assay (52) that was sensitive and could be adapted to measure Glu-AdT activity (92, 93). PfGluRS glutamylated apicoplast $tRNA^{Glu}$ and $tRNA^{Gln}$, but not cytoplasmic $tRNA^{Glu}$, $tRNA^{Gln}$, or *E. coli* tRNA (Fig. 4, *B* and *C*). The aminoacylation activity was therefore both nondiscriminating and specific for the apicoplast tRNAs. The kinetic analyses showed that, like other nondiscriminating GluRSs (94), PfGluRS-catalyzed glutamylation of the cognate and noncognate substrates at similar rates (Table 2). We also found that PfGluRS was sensitive to oxidation because DTT was required to maintain enzyme activity. The sensitivity of PfGluRS to oxidation might provide a means to regulate apicoplast protein synthesis in response to changes in the organelle's redox status (95).

As with other aaRSs (52), PfGluRS-catalyzed glutamylation was subject to product inhibition by PP_i, which was reversed by adding PPase to the reaction (Fig. 5*B*). Aminoacylation of tRNAs proceeds in two steps. First, the tRNA synthetase binds ATP and amino acid to form an enzyme-bound aminoacyl-adenylate and PP_i. Second, upon binding of the tRNA substrate to the enzyme-aminoacyl-adenylate complex, the amino acid is transferred from the aminoacyl-adenylate to the 3′ end of the tRNA with the concomitant release of PP_i. Subsequent PP_i hydrolysis provides a thermodynamic push for the reaction, so PP_i must be removed to prevent aaRS inhibition. Inorganic pyrophosphatase performs this function *in vivo*. PPase is essential in *E. coli* (96) and yeast (97), and chloroplasts possess a plastid-specific PPase. Transient repression of plastid PPase expression in tobacco leaves increased PP_i levels, reduced total soluble leaf protein by 60%, and inhibited expression of nucleus- and plastid-encoded subunits of the carbon-fixing enzyme ribulose-1,5-bisphosphate carboxylase oxygenase, suggesting that repressing plastid PPase levels reduced cytoplasmic and plastid protein synthesis (98). The *P. falciparum* genome (99)

encodes a soluble pyrophosphatase (PF3D7_0316300) that may be dual-targeted to the apicoplast and the cytoplasm via two alternatively spliced isoforms. The enzyme is expressed in asexual stages and gametocytes (71, 100); an apicoplast isoform might regulate PP_i levels within the organelle to prevent PP_i-mediated inhibition of protein synthesis or PP_i-sensitive enzymes in pathways such as isoprenoid biosynthesis (13).

Next, we tested whether a potent bacterial GluRS inhibitor, Glu-SA, was able to inhibit the *Plasmodium* enzyme. Glu-SA inhibited PfGluRS activity ($K_i = 0.7\ \mu$M, Fig. 6) but with a 250- and 10-fold lower efficiency than for *E. coli* or murine liver GluRSs, respectively (59). The wide range of susceptibility to Glu-SA inhibition exhibited by enzymes from different lineages probably reflects structural differences between their active sites. These differences between *Plasmodium* and host enzymes might be exploited to produce inhibitors with selective activity against the *Plasmodium* apicoplast GluRS.

The PfGluRS and its apicomplexan orthologs possess a bipartite apicoplast targeting sequence, but the enzyme's subcellular localization had never been determined experimentally. We found via immunofluorescence microscopy of Myc-tagged PbGluRS that the enzyme was localized in the apicoplast in erythrocytic stage parasites (Fig. 8*A*). Minor overlaps between the anti-Myc and MitoTracker Red signals were observed where the apicoplast and mitochondrion appeared to contact one another (Fig. 8*B*), a phenomenon observed with other apicoplast-targeted proteins (86, 101). Localization of PbGluRS solely in the apicoplast differs from the situation in *Arabidopsis*, where at least 15 nucleus-encoded aaRSs, including GluRS, are targeted to the plastid and the mitochondrion (102). Plasmodial genomes encode a second GluRS in addition to the one studied here, but that enzyme, encoded *in P. falciparum* by the gene Pf3D7_1349200, is predicted to be cytoplasmic (66, 68, 88). Dual targeting of aaRSs to the plastid and mitochondrion is common in higher plants (102), but this is unlikely in *Plasmodium* because the mitochondrion in the related parasite *Toxoplasma* imports aminoacylated tRNAs from the cytoplasm (66).

In this work, we identified components of an indirect aminoacylation pathway to produce Gln-$tRNA^{Gln}$ for apicoplast protein synthesis. We demonstrated that the first enzyme in the pathway, GluRS, is targeted to the apicoplast in blood stage parasites and can glutamylate both $tRNA^{Glu}$ and $tRNA^{Gln}$ *in vitro*. The latter property is associated with GluRSs that play a role in indirect aminoacylation, providing convincing evidence that the apicoplast indeed uses this pathway. The second enzyme in the pathway, Glu-AdT, has not been studied in *Plasmodium*, but we have expressed recombinant *P. falciparum* GatA and GatB subunits[5] and are testing whether they can amidate Glu-$tRNA^{Gln}$ produced by the PfGluRS to form Gln-$tRNA^{Gln}$. We are also investigating a potential novel feature of the *Plasmodium* Glu-AdT, the apparent absence of a GatC subunit that is required to stabilize the bacterial Glu-AdT (GatCAB) (69, 103), and whether the GluRS, Glu-AdT, and $tRNA^{Gln}$ form a ribonucleoprotein complex (the transamidosome) as they do in bacteria (104–106). Finally, apicoplast indirect aminoacylation is probably essential in malaria parasites because the parasite genome does not encode an apicoplast-targeted GlnRS (66, 68, 88). This is consistent with our inability to delete the gene encoding the *P. berghei* apicoplast GluRS in three independent experiments, despite the fact that it was accessible to *myc* tagging. This pathway may be a potential drug target because apicoplast protein synthesis is essential in both blood and liver stages. Further investigations to examine the requirements for apicoplast indirect aminoacylation across the *Plasmodium* life cycle and to identify specific inhibitors of plasmodial GluRS or Glu-AdT enzymes may lead to novel ways in which to target this pathway for chemotherapy.

Acknowledgments—We thank Geoffrey McFadden for providing anti-ACP antibody, J. Lapointe, and A. Weiner for plasmids expressing E. coli glutamyl-tRNA synthetase and CCA-adding enzyme, Y. M. Hou for the pGFIB vector, and Kelly Sheppard, A. Vaughan, and S. Mikolajczak for advice. We thank MR4 for providing P. falciparum 3D7 parasites contributed by Dan Carucci and Alister Craig. Unpublished P. berghei genome sequence data were produced by the Pathogen Sequencing Group at the Wellcome Trust Sanger Institute and can be obtained on line.

REFERENCES

1. World Health Organization (2012) *World Malaria Report 2012,* World Health Organization, Geneva
2. Murray, C. J., Rosenfeld, L. C., Lim, S. S., Andrews, K. G., Foreman, K. J., Haring, D., Fullman, N., Naghavi, M., Lozano, R., and Lopez, A. D. (2012) Global malaria mortality between 1980 and 2010: a systematic analysis. *Lancet* **379,** 413–431
3. Dondorp, A. M., Nosten, F., Yi, P., Das, D., Phyo, A. P., Tarning, J., Lwin, K. M., Ariey, F., Hanpithakpong, W., Lee, S. J., Ringwald, P., Silamut, K., Imwong, M., Chotivanich, K., Lim, P., Herdman, T., An, S. S., Yeung, S., Singhasivanon, P., Day, N. P., Lindegardh, N., Socheat, D., and White, N. J. (2009) Artemisinin resistance in *Plasmodium falciparum* malaria. *N. Engl. J. Med.* **361,** 455–467
4. McFadden, G. I., Reith, M. E., Munholland, J., and Lang-Unnasch, N. (1996) Plastid in human parasites. *Nature* **381,** 482–483
5. Wilson, R. J., Denny, P. W., Preiser, P. R., Rangachari, K., Roberts, K., Roy, A., Whyte, A., Strath, M., Moore, D. J., Moore, P. W., and Williamson, D. H. (1996) Complete gene map of the plastid-like DNA of the malaria parasite *Plasmodium falciparum*. *J. Mol. Biol.* **261,** 155–172
6. Gardner, M. J., Feagin, J. E., Moore, D. J., Spencer, D. F., Gray, M. W., Williamson, D. H., and Wilson, R. J. (1991) Organization and expression of small subunit ribosomal RNA genes encoded by a 35-kb circular DNA in *Plasmodium falciparum*. *Mol. Biochem. Parasitol.* **48,** 77–88
7. Gardner, M. J., Williamson, D. H., and Wilson, R. J. (1991) A circular DNA in malaria parasites encodes an RNA polymerase like that of prokaryotes and chloroplasts. *Mol. Biochem. Parasitol.* **44,** 115–123
8. Seeber, F. (2002) Biogenesis of iron-sulphur clusters in amitochondriate and apicomplexan protists. *Int. J. Parasitol.* **32,** 1207–1217
9. Waller, R. F., Keeling, P. J., Donald, R. G., Striepen, B., Handman, E., Lang-Unnasch, N., Cowman, A. F., Besra, G. S., Roos, D. S., and McFadden, G. I. (1998) Nuclear-encoded proteins target to the plastid in *Toxoplasma gondii* and *Plasmodium falciparum*. *Proc. Natl. Acad. Sci. U.S.A.* **95,** 12352–12357
10. Gardner, M. J., Hall, N., Fung, E., White, O., Berriman, M., Hyman, R. W., Carlton, J. M., Pain, A., Nelson, K. E., Bowman, S., Paulsen, I. T., James, K., Eisen, J. A., Rutherford, K., Salzberg, S. L., Craig, A., Kyes, S., Chan, M. S., Nene, V., Shallom, S. J., Suh, B., Peterson, J., Angiuoli, S., Pertea, M., Allen, J., Selengut, J., Haft, D., Mather, M. W., Vaidya, A. B., Martin, D. M., Fairlamb, A. H., Fraunholz, M. J., Roos, D. S., Ralph, S. A., McFadden, G. I., Cummings, L. M., Subramanian, G. M., Mungall, C., Venter, J. C., Carucci, D. J., Hoffman, S. L., Newbold, C., Davis, R. W., Fraser, C. M., and Barrell, B. (2002) Genome sequence of the human malaria parasite *Plasmodium falciparum*. *Nature* **419,** 498–511
11. Ralph, S. A., van Dooren, G. G., Waller, R. F., Crawford, M. J., Fraunholz,

M. J., Foth, B. J., Tonkin, C. J., Roos, D. S., and McFadden, G. I. (2004) Metabolic maps and functions of the *Plasmodium falciparum* apicoplast. *Nat. Rev. Microbiol.* **2,** 203–216

12. Gardner, M. J., Tettelin, H., Carucci, D. J., Cummings, L. M., Aravind, L., Koonin, E. V., Shallom, S., Mason, T., Yu, K., Fujii, C., Pederson, J., Shen, K., Jing, J., Aston, C., Lai, Z., Schwartz, D. C., Pertea, M., Salzberg, S., Zhou, L., Sutton, G. G., Clayton, R., White, O., Smith, H. O., Fraser, C. M., Adams, M. D., Venter, J. C., and Hoffman, S. L. (1998) Chromosome 2 sequence of the human malaria parasite *Plasmodium falciparum*. *Science* **282,** 1126–1132
13. Jomaa, H., Wiesner, J., Sanderbrand, S., Altincicek, B., Weidemeyer, C., Hintz, M., Türbachova, I., Eberl, M., Zeidler, J., Lichtenthaler, H. K., Soldati, D., and Beck, E. (1999) Inhibitors of the nonmevalonate pathway of isoprenoid biosynthesis as antimalarial drugs. *Science* **285,** 1573–1576
14. Nagaraj, V. A., Arumugam, R., Chandra, N. R., Prasad, D., Rangarajan, P. N., and Padmanaban, G. (2009) Localisation of *Plasmodium falciparum* uroporphyrinogen III decarboxylase of the heme-biosynthetic pathway in the apicoplast and characterisation of its catalytic properties. *Int. J. Parasitol.* **39,** 559–568
15. Günther, S., Matuschewski, K., and Müller, S. (2009) Knockout studies reveal an important role of *Plasmodium* lipoic acid protein ligase A1 for asexual blood stage parasite survival. *PLoS One* **4,** e5510
16. Vaughan, A. M., O'Neill, M. T., Tarun, A. S., Camargo, N., Phuong, T. M., Aly, A. S., Cowman, A. F., and Kappe, S. H. (2009) Type II fatty acid synthesis is essential only for malaria parasite late liver stage development. *Cell. Microbiol.* **11,** 506–520
17. Yeh, E., and DeRisi, J. L. (2011) Chemical rescue of malaria parasites lacking an apicoplast defines organelle function in blood-stage *Plasmodium falciparum*. *PLoS Biol.* **9,** e1001138
18. Goodman, C. D., and McFadden, G. I. (2013) Targeting apicoplasts in malaria parasites. *Expert Opin. Ther. Targets* **17,** 167–177
19. Geary, T. G., and Jensen, J. B. (1983) Effects of antibiotics on *Plasmodium falciparum in vitro*. *Am. J. Trop. Med. Hyg.* **32**, 221–225
20. Ginsburg, H., Divo, A. A., Geary, T. G., Boland, M. T., and Jensen, J. B. (1986) Effects of mitochondrial inhibitors on intraerythrocytic *Plasmodium falciparum* in *in vitro* cultures. *J. Protozool.* **33,** 121–125
21. Puri, S. K., and Singh, N. (2000) Azithromycin: antimalarial profile against blood- and sporozoite-induced infections in mice and monkeys. *Exp. Parasitol.* **94,** 8–14
22. Sullivan, M., Li, J., Kumar, S., Rogers, M. J., and McCutchan, T. F. (2000) Effects of interruption of apicoplast function on malaria infection, development, and transmission. *Mol. Biochem. Parasitol.* **109,** 17–23
23. World Health Organization (2010) *Guidelines for the Treatment of Malaria,* 2nd Ed., pp. 53–62, World Health Organization, Geneva
24. Tan, K. R., Magill, A. J., Parise, M. E., and Arguin, P. M. (2011) Doxycycline for malaria chemoprophylaxis and treatment: report from the CDC expert meeting on malaria chemoprophylaxis. *Am. J. Trop. Med. Hyg.* **84,** 517–531
25. Dahl, E. L., and Rosenthal, P. J. (2008) Apicoplast translation, transcription and genome replication: targets for antimalarial antibiotics. *Trends Parasitol.* **24,** 279–284
26. Lv, P. C., and Zhu, H. L. (2012) Aminoacyl-tRNA synthetase inhibitors as potent antibacterials. *Curr. Med. Chem.* **19,** 3550–3563
27. Baker, S. J., Zhang, Y. K., Akama, T., Lau, A., Zhou, H., Hernandez, V., Mao, W., Alley, M. R., Sanders, V., and Plattner, J. J. (2006) Discovery of a new boron-containing antifungal agent, 5-fluoro-1,3-dihydro-1-hydroxy-2,1-benzoxaborole (AN2690), for the potential treatment of onychomycosis. *J. Med. Chem.* **49,** 4447–4450
28. Hoen, R., Novoa, E. M., López, A., Camacho, N., Cubells, L., Vieira, P., Santos, M., Marin-Garcia, P., Bautista, J. M., Cortés, A., Ribas de Pouplana, L., and Royo, M. (2013) Selective inhibition of an apicoplastic aminoacyl-tRNA synthetase from *Plasmodium falciparum*. *Chembiochem* **14,** 499–509
29. Bour, T., Akaddar, A., Lorber, B., Blais, S., Balg, C., Candolfi, E., and Frugier, M. (2009) Plasmodial aspartyl-tRNA synthetases and peculiarities in *Plasmodium falciparum*. *J. Biol. Chem.* **284,** 18893–18903
30. Hoepfner, D., McNamara, C. W., Lim, C. S., Studer, C., Riedl, R., Aust, T., McCormack, S. L., Plouffe, D. M., Meister, S., Schuierer, S., Plikat, U., Hartmann, N., Staedtler, F., Cotesta, S., Schmitt, E. K., Petersen, F., Supek, F., Glynne, R. J., Tallarico, J. A., Porter, J. A., Fishman, M. C., Bodenreider, C., Diagana, T. T., Movva, N. R., and Winzeler, E. A. (2012) Selective and specific inhibition of the *Plasmodium falciparum* lysyl-tRNA synthetase by the fungal secondary metabolite cladosporin. *Cell Host Microbe* **11,** 654–663
31. Khan, S., Garg, A., Camacho, N., Van Rooyen, J., Kumar Pole, A., Belrhali, H., Ribas de Pouplana, L., Sharma, V., and Sharma, A. (2013) Structural analysis of malaria-parasite lysyl-tRNA synthetase provides a platform for drug development. *Acta Crystallogr. D Biol. Crystallogr.* **69,** 785–795
32. Koh, C. Y., Kim, J. E., Napoli, A. J., Verlinde, C. L., Fan, E., Buckner, F. S., Van Voorhis, W. C., and Hol, W. G. (2013) Crystal structures of *Plasmodium falciparum* cytosolic tryptophanyl-tRNA synthetase and its potential as a target for structure-guided drug design. *Mol. Biochem. Parasitol.* **189,** 26–32
33. Khan, S., Garg, A., Sharma, A., Camacho, N., Picchioni, D., Saint-Léger, A., Ribas de Pouplana, L., Yogavel, M., and Sharma, A. (2013) An appended domain results in an unusual architecture for malaria parasite tryptophanyl-tRNA synthetase. *PLoS One* **8,** e66224
34. Sheppard, K., Yuan, J., Hohn, M. J., Jester, B., Devine, K. M., and Söll, D. (2008) From one amino acid to another: tRNA-dependent amino acid biosynthesis. *Nucleic Acids Res.* **36,** 1813–1825
35. Baick, J. W., Yoon, J. H., Namgoong, S., Söll, D., Kim, S. I., Eom, S. H., and Hong, K. W. (2004) Growth inhibition of *Escherichia coli* during heterologous expression of *Bacillus subtilis* glutamyl-tRNA synthetase that catalyzes the formation of mischarged glutamyl-tRNA1 Gln. *J. Microbiol.* **42,** 111–116
36. Carlton, J. M., Angiuoli, S. V., Suh, B. B., Kooij, T. W., Pertea, M., Silva, J. C., Ermolaeva, M. D., Allen, J. E., Selengut, J. D., Koo, H. L., Peterson, J. D., Pop, M., Kosack, D. S., Shumway, M. F., Bidwell, S. L., Shallom, S. J., van Aken, S. E., Riedmuller, S. B., Feldblyum, T. V., Cho, J. K., Quackenbush, J., Sedegah, M., Shoaibi, A., Cummings, L. M., Florens, L., Yates, J. R., Raine, J. D., Sinden, R. E., Harris, M. A., Cunningham, D. A., Preiser, P. R., Bergman, L. W., Vaidya, A. B., van Lin, L. H., Janse, C. J., Waters, A. P., Smith, H. O., White, O. R., Salzberg, S. L., Venter, J. C., Fraser, C. M., Hoffman, S. L., Gardner, M. J., and Carucci, D. J. (2002) Genome sequence and comparative analysis of the model rodent malaria parasite *Plasmodium yoelii yoelii*. *Nature* **419,** 512–519
37. Carlton, J. M., Adams, J. H., Silva, J. C., Bidwell, S. L., Lorenzi, H., Caler, E., Crabtree, J., Angiuoli, S. V., Merino, E. F., Amedeo, P., Cheng, Q., Coulson, R. M., Crabb, B. S., Del Portillo, H. A., Essien, K., Feldblyum, T. V., Fernandez-Becerra, C., Gilson, P. R., Gueye, A. H., Guo, X., Kang'a, S., Kooij, T. W., Korsinczky, M., Meyer, E. V., Nene, V., Paulsen, I., White, O., Ralph, S. A., Ren, Q., Sargeant, T. J., Salzberg, S. L., Stoeckert, C. J., Sullivan, S. A., Yamamoto, M. M., Hoffman, S. L., Wortman, J. R., Gardner, M. J., Galinski, M. R., Barnwell, J. W., and Fraser-Liggett, C. M. (2008) Comparative genomics of the neglected human malaria parasite *Plasmodium vivax*. *Nature* **455,** 757–763
38. Gardner, M. J., Bishop, R., Shah, T., de Villiers, E. P., Carlton, J. M., Hall, N., Ren, Q., Paulsen, I. T., Pain, A., Berriman, M., Wilson, R. J., Sato, S., Ralph, S. A., Mann, D. J., Xiong, Z., Shallom, S. J., Weidman, J., Jiang, L., Lynn, J., Weaver, B., Shoaibi, A., Domingo, A. R., Wasawo, D., Crabtree, J., Wortman, J. R., Haas, B., Angiuoli, S. V., Creasy, T. H., Lu, C., Suh, B., Silva, J. C., Utterback, T. R., Feldblyum, T. V., Pertea, M., Allen, J., Nierman, W. C., Taracha, E. L., Salzberg, S. L., White, O. R., Fitzhugh, H. A., Morzaria, S., Venter, J. C., Fraser, C. M., and Nene, V. (2005) Genome sequence of *Theileria parva*, a bovine pathogen that transforms lymphocytes. *Science* **309,** 134–137
39. Hall, N., Karras, M., Raine, J. D., Carlton, J. M., Kooij, T. W., Berriman, M., Florens, L., Janssen, C. S., Pain, A., Christophides, G. K., James, K., Rutherford, K., Harris, B., Harris, D., Churcher, C., Quail, M. A., Ormond, D., Doggett, J., Trueman, H. E., Mendoza, J., Bidwell, S. L., Rajandream, M. A., Carucci, D. J., Yates, J. R., 3rd, Kafatos, F. C., Janse, C. J., Barrell, B., Turner, C. M., Waters, A. P., and Sinden, R. E. (2005) A comprehensive survey of the *Plasmodium* life cycle by genomic, transcriptomic, and proteomic analyses. *Science* **307,** 82–86
40. Aurrecoechea, C., Brestelli, J., Brunk, B. P., Dommer, J., Fischer, S., Gajria, B., Gao, X., Gingle, A., Grant, G., Harb, O. S., Heiges, M., Innamorato, F., Iodice, J., Kissinger, J. C., Kraemer, E., Li, W., Miller, J. A., Nayak, V., Pennington, C., Pinney, D. F., Roos, D. S., Ross, C., Stoeckert, C. J., Jr.,

Treatman, C., and Wang, H. (2009) PlasmoDB: a functional genomic database for malaria parasites. *Nucleic Acids Res.* **37,** D539–D543
41. UniProt Consortium (2010) *The Universal Protein Resource* (*UniProt*) *in 2010. Nucleic Acids Res.* **38,** D142–D148
42. Armougom, F., Moretti, S., Poirot, O., Audic, S., Dumas, P., Schaeli, B., Keduas, V., and Notredame, C. (2006) Expresso: automatic incorporation of structural information in multiple sequence alignments using 3D-Coffee. *Nucleic Acids Res.* **34,** W604–W608
43. Gouet, P., Courcelle, E., Stuart, D. I., and Métoz, F. (1999) ESPript: analysis of multiple sequence alignments in PostScript. *Bioinformatics* **15,** 305–308
44. Dereeper, A., Guignon, V., Blanc, G., Audic, S., Buffet, S., Chevenet, F., Dufayard, J. F., Guindon, S., Lefort, V., Lescot, M., Claverie, J. M., and Gascuel, O. (2008) Phylogeny.fr: robust phylogenetic analysis for the non-specialist. *Nucleic Acids Res.* **36,** W465–W469
45. Edgar, R. C. (2004) MUSCLE: a multiple sequence alignment method with reduced time and space complexity. *BMC Bioinformatics* **5,** 113
46. Castresana, J. (2000) Selection of conserved blocks from multiple alignments for their use in phylogenetic analysis. *Mol. Biol. Evol.* **17,** 540–552
47. Guindon, S., and Gascuel, O. (2003) A simple, fast, and accurate algorithm to estimate large phylogenies by maximum likelihood. *Syst. Biol.* **52,** 696–704
48. Chevenet, F., Brun, C., Bañuls, A. L., Jacq, B., and Christen, R. (2006) TreeDyn: towards dynamic graphics and annotations for analyses of trees. *BMC Bioinformatics* **7,** 439
49. Trager, W., and Jensen, J. B. (1976) Human malaria parasites in continuous culture. *Science* **193,** 673–675
50. Mudeppa, D. G., Pang, C. K., Tsuboi, T., Endo, Y., Buckner, F. S., Varani, G., and Rathod, P. K. (2007) Cell-free production of functional *Plasmodium falciparum* dihydrofolate reductase-thymidylate synthase. *Mol. Biochem. Parasitol.* **151,** 216–219
51. Jortzik, E., Mailu, B. M., Preuss, J., Fischer, M., Bode, L., Rahlfs, S., and Becker, K. (2011) Glucose-6-phosphate dehydrogenase 6-phosphogluconolactonase: a unique bifunctional enzyme from *Plasmodium falciparum*. *Biochem. J.* **436,** 641–650
52. Wolfson, A. D., and Uhlenbeck, O. C. (2002) Modulation of tRNAAla identity by inorganic pyrophosphatase. *Proc. Natl. Acad. Sci. U.S.A.* **99,** 5965–5970
53. Masson, J. M., and Miller, J. H. (1986) Expression of synthetic suppressor tRNA genes under the control of a synthetic promoter. *Gene* **47,** 179–183
54. Jahn, C. E., Charkowski, A. O., and Willis, D. K. (2008) Evaluation of isolation methods and RNA integrity for bacterial RNA quantitation. *J. Microbiol. Methods* **75,** 318–324
55. Oshikane, H., Sheppard, K., Fukai, S., Nakamura, Y., Ishitani, R., Numata, T., Sherrer, R. L., Feng, L., Schmitt, E., Panvert, M., Blanquet, S., Mechulam, Y., Söll, D., and Nureki, O. (2006) Structural basis of RNA-dependent recruitment of glutamine to the genetic code. *Science* **312,** 1950–1954
56. Dubois, D. Y., Blais, S. P., Huot, J. L., and Lapointe, J. (2009) A C-truncated glutamyl-tRNA synthetase specific for tRNA(Glu) is stimulated by its free complementary distal domain: mechanistic and evolutionary implications. *Biochemistry* **48,** 6012–6021
57. Feng, L., Sheppard, K., Tumbula-Hansen, D., and Söll, D. (2005) Gln-tRNAGln formation from Glu-tRNAGln requires cooperation of an asparaginase and a Glu-tRNAGln kinase. *J. Biol. Chem.* **280,** 8150–8155
58. Freist, W., Sternbach, H., and Cramer, F. (1989) Arginyl-tRNA synthetase from yeast. Discrimination between 20 amino acids in aminoacylation of tRNA(Arg)-C-C-A and tRNA(Arg)-C-C-A(3′NH2). *Eur. J. Biochem.* **186,** 535–541
59. Bernier, S., Dubois, D. Y., Habegger-Polomat, C., Gagnon, L.-P., Lapointe, J., and Chênevert, R. (2005) Glutamylsulfamoyladenosine and pyroglutamylsulfamoyladenosine are competitive inhibitors of *E. coli* glutamyl-tRNA synthetase. *J. Enzyme Inhib. Med. Chem.* **20,** 61–67
60. Mikolajczak, S. A., Aly, A. S., Dumpit, R. F., Vaughan, A. M., and Kappe, S. H. (2008) An efficient strategy for gene targeting and phenotypic assessment in the *Plasmodium yoelii* rodent malaria model. *Mol. Biochem. Parasitol.* **158,** 213–216
61. Labaied, M., Harupa, A., Dumpit, R. F., Coppens, I., Mikolajczak, S. A., and Kappe, S. H. (2007) *Plasmodium yoelii* sporozoites with simultaneous deletion of P52 and P36 are completely attenuated and confer sterile immunity against infection. *Infect. Immun.* **75,** 3758–3768
62. Tonkin, C. J., van Dooren, G. G., Spurck, T. P., Struck, N. S., Good, R. T., Handman, E., Cowman, A. F., and McFadden, G. I. (2004) Localization of organellar proteins in *Plasmodium falciparum* using a novel set of transfection vectors and a new immunofluorescence fixation method. *Mol. Biochem. Parasitol.* **137,** 13–21
63. Waller, R. F., Reed, M. B., Cowman, A. F., and McFadden, G. I. (2000) Protein trafficking to the plastid of *Plasmodium falciparum* is via the secretory pathway. *EMBO J.* **19,** 1794–1802
64. Zuegge, J., Ralph, S., Schmuker, M., McFadden, G. I., and Schneider, G. (2001) Deciphering apicoplast targeting signals–feature extraction from nuclear-encoded precursors of *Plasmodium falciparum* apicoplast proteins. *Gene* **280,** 19–26
65. Foth, B. J., Ralph, S. A., Tonkin, C. J., Struck, N. S., Fraunholz, M., Roos, D. S., Cowman, A. F., and McFadden, G. I. (2003) Dissecting apicoplast targeting in the malaria parasite *Plasmodium falciparum*. *Science* **299,** 705–708
66. Pino, P., Aeby, E., Foth, B. J., Sheiner, L., Soldati, T., Schneider, A., and Soldati-Favre, D. (2010) Mitochondrial translation in absence of local tRNA aminoacylation and methionyl tRNA Met formylation in *Apicomplexa*. *Mol. Microbiol.* **76,** 706–718
67. Saad, N. Y., Schiel, B., Brayé, M., Heap, J. T., Minton, N. P., Dürre, P., and Becker, H. D. (2012) Riboswitch (T-box)-mediated control of tRNA-dependent amidation in *Clostridium acetobutylicum* rationalizes gene and pathway redundancy for asparagine and asparaginyl-trnaasn synthesis. *J. Biol. Chem.* **287,** 20382–20394
68. Jackson, K. E., Habib, S., Frugier, M., Hoen, R., Khan, S., Pham, J. S., Ribas de Pouplana, L., Royo, M., Santos, M. A., Sharma, A., and Ralph, S. A. (2011) Protein translation in *Plasmodium* parasites. *Trends Parasitol.* **27,** 467–476
69. Nakamura, A., Yao, M., Chimnaronk, S., Sakai, N., and Tanaka, I. (2006) Ammonia channel couples glutaminase with transamidase reactions in GatCAB. *Science* **312,** 1954–1958
70. Frechin, M., Senger, B., Brayé, M., Kern, D., Martin, R. P., and Becker, H. D. (2009) Yeast mitochondrial Gln-tRNA(Gln) is generated by a GatFAB-mediated transamidation pathway involving Arc1p-controlled subcellular sorting of cytosolic GluRS. *Genes Dev.* **23,** 1119–1130
71. Bozdech, Z., Llinas, M., Pulliam, B. L., Wong, E. D., Zhu, J., and DeRisi, J. L. (2003) The transcriptome of the intraerythrocytic developmental cycle of *Plasmodium falciparum*. *PLoS Biol.* Oct;1(1):E5
72. Vignali, M., Armour, C. D., Chen, J., Morrison, R., Castle, J. C., Biery, M. C., Bouzek, H., Moon, W., Babak, T., Fried, M., Raymond, C. K., and Duffy, P. E. (2011) NSR-seq transcriptional profiling enables identification of a gene signature of *Plasmodium falciparum* parasites infecting children. *J. Clin. Invest.* **121,** 1119–1129
73. Lasonder, E., Ishihama, Y., Andersen, J. S., Vermunt, A. M., Pain, A., Sauerwein, R. W., Eling, W. M., Hall, N., Waters, A. P., Stunnenberg, H. G., and Mann, M. (2002) Analysis of the *Plasmodium falciparum* proteome by high-accuracy mass spectrometry. *Nature* **419,** 537–542
74. Florens, L., Washburn, M. P., Raine, J. D., Anthony, R. M., Grainger, M., Haynes, J. D., Moch, J. K., Muster, N., Sacci, J. B., Tabb, D. L., Witney, A. A., Wolters, D., Wu, Y., Gardner, M. J., Holder, A. A., Sinden, R. E., Yates, J. R., and Carucci, D. J. (2002) A proteomic view of the *Plasmodium falciparum* life cycle. *Nature* **419,** 520–526
75. Eriani, G., Delarue, M., Poch, O., Gangloff, J., and Moras, D. (1990) Partition of tRNA synthetases into two classes based on mutually exclusive sets of sequence motifs. *Nature* **347,** 203–206
76. Sekine, S., Nureki, O., Dubois, D. Y., Bernier, S., Chênevert, R., Lapointe, J., Vassylyev, D. G., and Yokoyama, S. (2003) ATP binding by glutamyl-tRNA synthetase is switched to the productive mode by tRNA binding. *EMBO J.* **22,** 676–688
77. Banerjee, R., Dubois, D. Y., Gauthier, J., Lin, S. X., Roy, S., and Lapointe, J. (2004) The zinc-binding site of a class I aminoacyl-tRNA synthetase is a SWIM domain that modulates amino acid binding via the tRNA acceptor arm. *Eur. J. Biochem.* **271,** 724–733

78. Schulze, J. O., Masoumi, A., Nickel, D., Jahn, M., Jahn, D., Schubert, W. D., and Heinz, D. W. (2006) Crystal structure of a non-discriminating glutamyl-tRNA synthetase. *J. Mol. Biol.* **361,** 888–897
79. Shu, N., Zhou, T., and Hovmöller, S. (2008) Prediction of zinc-binding sites in proteins from sequence. *Bioinformatics* **24,** 775–782
80. Lee, J., and Hendrickson, T. L. (2004) Divergent anticodon recognition in contrasting glutamyl-tRNA synthetases. *J. Mol. Biol.* **344,** 1167–1174
81. Sekine, S., Nureki, O., Shimada, A., Vassylyev, D. G., and Yokoyama, S. (2001) Structural basis for anticodon recognition by discriminating glutamyl-tRNA synthetase. *Nat. Struct. Biol.* **8,** 203–206
82. Bullock, T. L., Uter, N., Nissan, T. A., and Perona, J. J. (2003) Amino acid discrimination by a class I aminoacyl-tRNA synthetase specified by negative determinants. *J. Mol. Biol.* **328,** 395–408
83. Freist, W. (1989) Mechanisms of aminoacyl-tRNA synthetases: a critical consideration of recent results. *Biochemistry* **28,** 6787–6795
84. Brown, P., Richardson, C. M., Mensah, L. M., O'Hanlon, P. J., Osborne, N. F., Pope, A. J., and Walker, G. (1999) Molecular recognition of tyrosinyl adenylate analogues by prokaryotic tyrosyl tRNA synthetases. *Bioorg. Med. Chem.* **7,** 2473–2485
85. Hall, N., Pain, A., Berriman, M., Churcher, C., Harris, B., Harris, D., Mungall, K., Bowman, S., Atkin, R., Baker, S., Barron, A., Brooks, K., Buckee, C. O., Burrows, C., Cherevach, I., Chillingworth, C., Chillingworth, T., Christodoulou, Z., Clark, L., Clark, R., Corton, C., Cronin, A., Davies, R., Davis, P., Dear, P., Dearden, F., Doggett, J., Feltwell, T., Goble, A., Goodhead, I., Gwilliam, R., Hamlin, N., Hance, Z., Harper, D., Hauser, H., Hornsby, T., Holroyd, S., Horrocks, P., Humphray, S., Jagels, K., James, K. D., Johnson, D., Kerhornou, A., Knights, A., Konfortov, B., Kyes, S., Larke, N., Lawson, D., Lennard, N., Line, A., Maddison, M., McLean, J., Mooney, P., Moule, S., Murphy, L., Oliver, K., Ormond, D., Price, C., Quail, M. A., Rabbinowitsch, E., Rajandream, M. A., Rutter, S., Rutherford, K. M., Sanders, M., Simmonds, M., Seeger, K., Sharp, S., Smith, R., Squares, R., Squares, S., Stevens, K., Taylor, K., Tivey, A., Unwin, L., Whitehead, S., Woodward, J., Sulston, J. E., Craig, A., Newbold, C., and Barrell, B. G. (2002) Sequence of *Plasmodium falciparum* chromosomes 1, 3–9, and 13. *Nature* **419,** 527–531
86. van Dooren, G. G., Marti, M., Tonkin, C. J., Stimmler, L. M., Cowman, A. F., and McFadden, G. I. (2005) Development of the endoplasmic reticulum, mitochondrion and apicoplast during the asexual life cycle of *Plasmodium falciparum*. *Mol. Microbiol.* **57,** 405–419
87. Pedroni, M. J., Luu, T. N., and Lau, A. O. (2012) *Babesia bovis*: a bipartite signal directs the glutamyl-tRNA synthetase to the apicoplast. *Exp. Parasitol.* **131,** 261–266
88. Bhatt, T. K., Kapil, C., Khan, S., Jairajpuri, M. A., Sharma, V., Santoni, D., Silvestrini, F., Pizzi, E., and Sharma, A. (2009) A genomic glimpse of aminoacyl-tRNA synthetases in malaria parasite *Plasmodium falciparum*. *BMC Genomics* **10,** 644
89. Ilan, J., and Ilan, J. (1969) Aminoacyl transfer ribonucleic acid synthetases from cell-free extract of *Plasmodium berghei*. *Science* **164,** 560–562
90. Istvan, E. S., Dharia, N. V., Bopp, S. E., Gluzman, I., Winzeler, E. A., and Goldberg, D. E. (2011) Validation of isoleucine utilization targets in *Plasmodium falciparum*. *Proc. Natl. Acad. Sci. U.S.A.* **108,** 1627–1632
91. Jackson, K. E., Pham, J. S., Kwek, M., De Silva, N. S., Allen, S. M., Goodman, C. D., McFadden, G. I., de Pouplana, L. R., and Ralph, S. A. (2012) Dual targeting of aminoacyl-tRNA synthetases to the apicoplast and cytosol in *Plasmodium falciparum*. *Int. J. Parasitol.* **42,** 177–186
92. Sheppard, K., Akochy, P. M., Salazar, J. C., and Söll, D. (2007) The *Helicobacter pylori* amidotransferase GatCAB is equally efficient in glutamine-dependent transamidation of Asp-tRNAAsn and Glu-tRNAGln. *J. Biol. Chem.* **282,** 11866–11873
93. Sheppard, K., Akochy, P. M., and Söll, D. (2008) Assays for transfer RNA-dependent amino acid biosynthesis. *Methods* **44,** 139–145
94. Lapointe, J., Duplain, L., and Proulx, M. (1986) A single glutamyl-tRNA synthetase aminoacylates tRNAGlu and tRNAGln in *Bacillus subtilis* and efficiently misacylates *Escherichia coli* tRNAGln1 *in vitro*. *J. Bacteriol.* **165,** 88–93
95. Katz, A., Banerjee, R., de Armas, M., Ibba, M., and Orellana, O. (2010) Redox status affects the catalytic activity of glutamyl-tRNA synthetase. *Biochem. Biophys. Res. Commun.* **398,** 51–55
96. Chen, J., Brevet, A., Fromant, M., Lévêque, F., Schmitter, J. M., Blanquet, S., and Plateau, P. (1990) Pyrophosphatase is essential for growth of. *Escherichia coli*. *J. Bacteriol.* **172,** 5686–5689
97. Giaever, G., Chu, A. M., Ni, L., Connelly, C., Riles, L., Véronneau, S., Dow, S., Lucau-Danila, A., Anderson, K., André, B., Arkin, A. P., Astromoff, A., El-Bakkoury, M., Bangham, R., Benito, R., Brachat, S., Campanaro, S., Curtiss, M., Davis, K., Deutschbauer, A., Entian, K. D., Flaherty, P., Foury, F., Garfinkel, D. J., Gerstein, M., Gotte, D., Güldener, U., Hegemann, J. H., Hempel, S., Herman, Z., Jaramillo, D. F., Kelly, D. E., Kelly, S. L., Kötter, P., LaBonte, D., Lamb, D. C., Lan, N., Liang, H., Liao, H., Liu, L., Luo, C., Lussier, M., Mao, R., Menard, P., Ooi, S. L., Revuelta, J. L., Roberts, C. J., Rose, M., Ross-Macdonald, P., Scherens, B., Schimmack, G., Shafer, B., Shoemaker, D. D., Sookhai-Mahadeo, S., Storms, R. K., Strathern, J. N., Valle, G., Voet, M., Volckaert, G., Wang, C. Y., Ward, T. R., Wilhelmy, J., Winzeler, E. A., Yang, Y., Yen, G., Youngman, E., Yu, K., Bussey, H., Boeke, J. D., Snyder, M., Philippsen, P., Davis, R. W., and Johnston, M. (2002) Functional profiling of the *Saccharomyces cerevisiae* genome. *Nature* **418,** 387–391
98. George, G. M., van der Merwe, M. J., Nunes-Nesi, A., Bauer, R., Fernie, A. R., Kossmann, J., and Lloyd, J. R. (2010) Virus-induced gene silencing of plastidial soluble inorganic pyrophosphatase impairs essential leaf anabolic pathways and reduces drought stress tolerance in *Nicotiana benthamiana*. *Plant Physiol.* **154,** 55–66
99. Bowman, S., Lawson, D., Basham, D., Brown, D., Chillingworth, T., Churcher, C. M., Craig, A., Davies, R. M., Devlin, K., Feltwell, T., Gentles, S., Gwilliam, R., Hamlin, N., Harris, D., Holroyd, S., Hornsby, T., Horrocks, P., Jagels, K., Jassal, B., Kyes, S., McLean, J., Moule, S., Mungall, K., Murphy, L., Oliver, K., Quail, M. A., Rajandream, M. A., Rutter, S., Skelton, J., Squares, R., Squares, S., Sulston, J. E., Whitehead, S., Woodward, J. R., Newbold, C., and Barrell, B. G. (1999) The complete nucleotide sequence of chromosome 3 of *Plasmodium falciparum*. *Nature* **400,** 532–538
100. Young, J. A., Fivelman, Q. L., Blair, P. L., de la Vega, P., Le Roch, K. G., Zhou, Y., Carucci, D. J., Baker, D. A., and Winzeler, E. A. (2005) The *Plasmodium falciparum* sexual development transcriptome: a microarray analysis using ontology-based pattern identification. *Mol. Biochem. Parasitol.* **143,** 67–79
101. Hopkins, J., Fowler, R., Krishna, S., Wilson, I., Mitchell, G., and Bannister, L. (1999) The plastid in *Plasmodium falciparum* asexual blood stages: a three-dimensional ultrastructural analysis. *Protist.* **150,** 283–295
102. Duchêne, A. M., Giritch, A., Hoffmann, B., Cognat, V., Lancelin, D., Peeters, N. M., Zaepfel, M., Maréchal-Drouard, L., and Small, I. D. (2005) Dual targeting is the rule for organellar aminoacyl-tRNA synthetases in *Arabidopsis thaliana*. *Proc. Natl. Acad. Sci. U.S.A.* **102,** 16484–16489
103. Curnow, A. W., Hong Kw., Yuan, R., Kim Si., Martins, O., Winkler, W., Henkin, T. M., and Söll, D. (1997) Glu-tRNAGln amidotransferase: a novel heterotrimeric enzyme required for correct decoding of glutamine codons during translation. *Proc. Natl. Acad. Sci. U.S.A.* **94,** 11819–11826
104. Bailly, M., Blaise, M., Lorber, B., Becker, H. D., and Kern, D. (2007) The transamidosome: a dynamic ribonucleoprotein particle dedicated to prokaryotic tRNA-dependent asparagine biosynthesis. *Mol. Cell* **28,** 228–239
105. Ito, T., and Yokoyama, S. (2010) Two enzymes bound to one transfer RNA assume alternative conformations for consecutive reactions. *Nature* **467,** 612–616
106. Huot, J. L., Fischer, F., Corbeil, J., Madore, E., Lorber, B., Diss, G., Hendrickson, T. L., Kern, D., and Lapointe, J. (2011) Gln-tRNA^{Gln} synthesis in a dynamic transamidosome from *Helicobacter pylori*, where GluRS2 hydrolyzes excess Glu-tRNA^{Gln}. *Nucleic Acids Res.* **39,** 9306–9315
107. Liu, J., Gagnon, Y., Gauthier, J., Furenlid, L., L'Heureux, P. J., Auger, M., Nureki, O., Yokoyama, S., and Lapointe, J. (1995) The zinc-binding site of *Escherichia coli* glutamyl-tRNA synthetase is located in the acceptor-binding domain. Studies by extended x-ray absorption fine structure, molecular modeling, and site-directed mutagenesis. *J. Biol. Chem.* **270,** 15162–15169
108. Labaied, M., Camargo, N., and Kappe, S. H. (2007) Depletion of the *Plasmodium berghei* thrombospondin-related sporozoite protein reveals a role in host cell entry by sporozoites. *Mol. Biochem. Parasitol.* **153,** 158–166